about 28% homologous to the Fas ligand. TRAIL induces apoptosis in various malignant tumors, but is non-toxic to normal cells. These functions of TRAIL may lead to the promise of a molecular target agent. TRAIL receptors are classified into TRAIL-R1 (death receptor 4, DR4); TRAIL-R2 (death receptor 5, DR5); TRAIL-R3 (decoy receptor 1, DcR1); TRAIL-R4 (decoy receptor 2, DcR2) and osteoprotegerin (OPG). DRs 4 and 5 have an intracellular death domain to induce apoptosis through initiator and effector caspases, whereas DcRs 1 and 2 are decoy receptors that do not induce apoptosis (10). Differences in TRAIL receptor expressions possibly result in apoptosis induction only in malignant tumors. However, its detailed mechanism remains unclear.

The present study aimed to identify the immune cells on which MUC5AC acts using an immune cell-depleted animal model and analyze the suppression mechanism. Then, we investigated the tumor growth of MUC5AC-knockdown cells using nude mice depleted of neutrophils with an anti-Gr-1 antibody and SCID mice depleted of B and T cells.

To examine whether B cells act directly on the rejection of implanted MUC5AC-knockdown cells, we investigated the tumor growth of MUC5AC-knockdown and MUC5AC-expressing cells in SCID mice. The growth of MUC5AC-knockdown cells did not recover (Fig. 1A). In SCID mice, an investigation in the double implantation system demonstrated that the tumor growth of MUC5AC-expressing cells was increased irrespective of whether a primary tumor was present or absent (unpublished observation). However, such growth was not observed in nude mice (unpublished observation). This suggests that MUC5AC suppresses memory B-cell immune reactions that function during prolonged antitumor reactions or cell metastasis.

In an experiment with neutrophil-depleted model mice, the tumor growth of MUC5AC-knockdown cells, barely observed in the presence of neutrophils, was recovered to the same level as MUC5AC-expressing cells when neutrophils were depleted (Fig. 1C). This suggests that MUC5AC plays an important role in directly suppressing the antitumor effects of neutrophils. Additionally, IL-8 production, barely observed in MUC5AC-expressing cells, was significantly increased in MUC5AC-knockdown cells (Fig. 2). According to these results, neutrophil infiltration into a tumor inducing by IL-8 was found to exert antitumor effects. However, the mechanism by which MUC5AC-knockdown increases IL-8 production by tumor cells still remains unknown and should be investigated in a future study.

An apoptosis array was employed to examine why MUC5AC-expressing cells differed from MUC5AC-knockdown cells in their susceptibilities to apoptosis mediated by TRAIL. DR4/TRAIL-R1 and DR5/TRAIL-R2 were weakly expressed in the routine cultures of both cells. However, the addition of TRAIL increased the expressions of DR4/TRAIL-R1, DR5/TRAIL-R2 and active-caspase 3 (effector caspase) in MUC5AC-knockdown cells (Fig. 4). Future studies will be aimed at investigating how TRAIL increases death receptor expressions in MUC5AC-knockdown cells.

The caspase family of proteases is the ultimate effector of programmed cell death. Under ordinary circumstances, caspases are kept in check by the inhibitor of apoptosis proteins (IAPs) such as cIAP1, cIAP2, XIAP, NAIP, livin/ML-IAP, BRUCE/Apollon and survivin, which bind to and inactive caspases until they are needed. Caspases are overexpressed in tumors, but IAPs likewise are overexpressed. Therefore, failure to activate caspases could create resistance to apoptosis (24,25). Several studies show that MUC4 and ErbB2 are coexpressed in some tumor types such as the breast, non-small cell lung cancer, and pancreas. The possibility that MUC4 could elicit its anti-apoptotic effects by ErbB2, engaging a variety of signaling cascades to elicit cellular responses, such as proliferation and survival, has been suggested (26,27). Prostaglandin E_2 (PGE_2) synthesized by cyclooxygenase-2 (COX-2), overproduced in various malignancies, has also been reported to be associated with anti-apoptotic effects and increase survivin expression (28,29). It is believed that MUC5AC may have promoted the expression or action of IAPs in some way or MUC5AC may have formed a complex with a certain molecule and promoted tumor growth via suppression of tumor cell apoptosis.

In the present study, we established MUC5AC-knockdown cells using siRNA to elucidate the functions of MUC5AC, whose expression is increased in pancreatic cancer. IL-8 production was promoted in MUC5AC-knockdown cells. In addition, cell death was induced by TRAIL through the apoptosis pathway, suggesting reduced tumorigenicity *in vivo*. It was suggested that induction of neutrophil migration is weak in normal MUC5AC-producing pancreatic cancer cells because IL-8 production is low and apoptosis induction by neutrophil-derived TRAIL is blocked due to the presence of MUC5AC, and these conditions promote pancreatic cancer cell proliferation and growth *in vivo*, being involved in aggressive tumor formation. Our observations suggest that the very potent anti-apoptotic effects of MUC5AC allow tumor cells to escape key barriers to tumor progression. These studies add to the knowledge on the significance of MUC5AC expression in cancer cells.

Acknowledgements

This study was conducted at Kureha Corporation, Tokyo and Osaka City University, Osaka, Japan. Hirotaka Hoshi, Motoyuki Uchida and Hiroko Iijima are employees of Kureha Corporation, but the study presents no conflict of interest.

References

1. Wang Z, Song W, Aboukameel A, Mohammad M, Wang G, Banerjee S, Kong D, Wang S, Sarkar FH and Mohammad RM: TW-37, a small-molecule inhibitor of Bcl-2, inhibits cell growth and invasion in pancreatic cancer. Int J Cancer 123: 958-966, 2008.
2. Sheehan JK, Brazeau C, Kutay S, Pigeon H, Kirkham S, Howard M and Thornton DJ: Physical characterization of the MUC5AC mucin: a highly oligomeric glycoprotein whether isolated from cell culture or in vivo from respiratory mucous secretions. Biochem J 347: 37-44, 2000.
3. Hollingsworth MA and Swanson BJ: Mucins in cancer: protection and control of the cell surface. Nat Rev Cancer 4: 45-60, 2004.
4. Ho JJL, Crawley S, Pan PL, Farrelly ER and Kim YS: Secretion of MUC5AC mucin from pancreatic cancer cells in response to forskolin and VIP. Biochem Biophys Res Commun 294: 680-686, 2002.
5. Tecchio C, Huber V, Scapini P, Calzetti F, Margotto D, Todeschini G, Pilla L, Martinelli G, Pizzolo G, Rivoltini L and Cassatella MA: IFNalpha-stimulated neutrophils and monocytes release a soluble form of TNF-related apoptosis-inducing ligand (TRAIL/Apo-2 ligand) displaying apoptotic activity on leukemic cells. Blood 103: 3837-3844, 2004.

6. Stockmeyer B, Beyer T, Neuhuber W, Repp R, Kalden JR, Valerius T and Herrmann M: Polymorphonuclear granulocytes induce antibody-dependent apoptosis in human breast cancer cells. J Immunol 171: 5124-5129, 2003.
7. Challacombe JM, Suhrbier A, Parsons PG, Jones B, Hampson P, Kavanagh D, Rainger GE, Morris M, Lord JM, Le TT, Hoang-Le D and Ogbourne SM: Neutrophils are a key component of the antitumor efficacy of topical chemotherapy with ingenol-3-angelate. J Immunol 177: 8123-8132, 2006.
8. Koga Y, Matsuzaki A, Suminoe A, Hattori H and Hara T: Neutrophil-derived TNF-related apoptosis-inducing ligand (TRAIL): a novel mechanism of antitumor effect by neutrophils. Cancer Res 64: 1037-1043, 2004.
9. Kemp TJ, Ludwig AT, Earel JK, Moore JM, Vanoosten RL, Moses B, Leidal K, Nauseef WM and Griffith TS: Neutrophil stimulation with Mycobacterium bovis bacillus Calmette-Guérin (BCG) results in the release of functional soluble TRAIL/Apo-2L. Blood 106: 3474-3482, 2005.
10. de Vries EG, Gietema JA and de Jong S: Tumor necrosis factor-related apoptosis-inducing ligand pathway and its therapeutic implications. Clin Cancer Res 12: 2390-2393, 2006.
11. Voortman J, Resende TP, Abou El Hassan MA, Giaccone G and Kruyt FA: TRAIL therapy in non-small cell lung cancer cells: sensitization to death receptor-mediated apoptosis by proteasome inhibitor bortezomib. Mol Cancer Ther 6: 2103-2112, 2007.
12. Hoshi H, Sawada T, Uchida M, Saito H, Iijima H, Toda-Agetsuma M, Wada T, Yamazoe S, Tanaka H, Kimura K, Kakehashi A, Wei M, Hirakawa K and Wanibuchi H: Tumor-associated MUC5AC stimulates *in vivo* tumorigenicity of human pancreatic cancer. Int J Oncol 38: 619-627, 2011.
13. Hernandez-Ilizaliturri FJ, Jupudy V, Ostberg J, Oflazoglu E, Huberman A, Repasky E and Czuczman MS: Neutrophils contribute to the biological antitumor activity of rituximab in a non-Hodgkin's lymphoma severe combined immunodeficiency mouse model. Clin Cancer Res 9: 5866-5873, 2003.
14. Singh PK and Hollingsworth MA: Cell surface-associated mucins in signal transduction. Trends Cell Biol 16: 467-476, 2006.
15. Lane D, Côté M, Grondin R, Couture MC and Piché A: Acquired resistance to TRAIL-induced apoptosis in human ovarian cancer cells is conferred by increased turnover of mature caspase-3. Mol Cancer Ther 5: 509-521, 2006.
16. Lane D, Robert V, Grondin R, Rancourt C and Piché A: Malignant ascites protect against TRAIL-induced apoptosis by activating the PI3K/Akt pathway in human ovarian carcinoma cells. Int J Cancer 121: 1227-1237, 2007.
17. Di Carlo E, Forni G, Lollini P, Colombo MP, Modesti A and Musiani P: The intriguing role of polymorphonuclear neutrophils in antitumor reactions. Blood 97: 339-345, 2001.
18. Alvarez MJ, Prada F, Salvatierra E, Bravo AI, Lutzky VP, Carbone C, Pitossi FJ, Chuluyan HE and Podhajcer OL: Secreted protein acidic and rich in cysteine produced by human melanoma cells modulates polymorphonuclear leukocyte recruitment and antitumor cytotoxic capacity. Cancer Res 65: 5123-5132, 2005.
19. Chen YL, Chen SH, Wang JY and Yang BC: Fas ligand on tumor cells mediates inactivation of neutrophils. J Immunol 171: 1183-1191, 2003.
20. Sanford MA, Yan Y, Canfield SE, Hassan W, Selleck WA, Atkinson G, Chen SH and Hall SJ: Independent contributions of GR-1+ leukocytes and Fas/FasL interactions to induce apoptosis following interleukin-12 gene therapy in a metastatic model of prostate cancer. Hum Gene Ther 12: 1485-1498, 2001.
21. Niitsu N, Khori M, Hayama M, Kajiwara K, Higashihara M and Tamaru J: Phase I/II study of the rituximab-EPOCT regimen in combination with granulocyte colony-stimulating factor in patients with relapsed or refractory follicular lymphoma including evaluation of its cardiotoxicity using B-type natriuretic peptide and troponin T levels. Clin Cancer Res 11: 697-702, 2005.
22. Otten MA, Rudolph E, Dechant M, Tuk CW, Reijmers RM, Beelen RH, van de Winkel JG and van Egmond M: Immature neutrophils mediate tumor cell killing via IgA but not IgG Fc receptors. J Immunol 174: 5472-5480, 2005.
23. Wiley SR, Schooley K, Smolak PJ, Din WS, Huang CP, Nicholl JK, Sutherland GR, Smith TD, Rauch C, Smith CA and Goodwin RG: Identification and characterization of a new member of the TNF family that induces apoptosis. Immunity 3: 673-682, 1995.
24. Schimmer AD: Inhibition of apoptosis proteins: translating basic knowledge into clinical practice. Cancer Res 64: 7183-7190, 2004.
25. Wei Y, Fan T and Yu M: Inhibitor of apoptosis proteins and apoptosis. Acta Biochim Biophys Sin (Shanghai) 40: 278-288, 2009.
26. Komatsu M, Jepson S, Arango ME, Carraway CAC and Carraway KL: Muc4/sialomucin complex, an intramembrane modulator of ErbB2/HER2/Neu, potentiates primary tumor growth and suppresses apoptosis in a xenotransplanted tumor. Oncogene 20: 461-470, 2001.
27. Workman HC, Sweeney C, Carraway KL III: The membrane mucin Muc4 inhibits apoptosis induced by multiple insults via ErbB2-dependent and ErbB2-independent mechanisms. Cancer Res 69: 2845-2852, 2009.
28. Baratelli F, Krysan K, Heuzé-Vourc'h N, Zhu L, Escuadro B, Sharma S, Reckamp K, Dohadwala M and Dubinett SM: PGE2 confers survivin-dependent apoptosis resistance in human monocyte-derived dendritic cells. J Leukoc Biol 78: 555-564, 2005.
29. Leone V, di Palma A, Ricchi P, Acquaviva F, Giannouli M, Di Prisco AM, Iuliano F and Acquaviva AM: PGE2 inhibits apoptosis in human adenocarcinoma Caco-2 cell line through Ras-PI3K association and cAMP-dependent kinase A activation. Am J Physiol Gastrointest Liver Physiol 293: G673-G681, 2007.

Toxicology and Applied Pharmacology 273 (2013) 390–400

Contents lists available at ScienceDirect

Toxicology and Applied Pharmacology

journal homepage: www.elsevier.com/locate/ytaap

Mode of action of ethyl *tertiary*-butyl ether hepatotumorigenicity in the rat: Evidence for a role of oxidative stress via activation of CAR, PXR and PPAR signaling pathways

Anna Kakehashi [a,*], Akihiro Hagiwara [b], Norio Imai [b], Kasuke Nagano [c], Fukumi Nishimaki [d], Marcy Banton [e], Min Wei [a], Shoji Fukushima [a,f], Hideki Wanibuchi [a]

[a] Department of Pathology, Osaka City University Graduate School of Medicine, 1-4-3 Asahi-machi, Abeno-ku, Osaka 545-8585, Japan
[b] DIMS Institute of Medical Science, Inc., 64 Goura, Nishiazai, Azai-cho, Ichinomiya, Aichi 491-0113, Japan
[c] Nagano Toxicologic-Pathology Consulting, Ochiai, Hadano, Kanagawa 257-0025, Japan
[d] Biofuel Assessment Group, New Fuels Dept., Japan Petroleum Energy Center (JPEC), 4-3-9 Toranomon, Minato-ku, Tokyo 105-0001, Japan
[e] Toxicology and Risk Assessment, LyondellBasell Industries, LyondellBasell Corporate HSE/Product Safety, One Houston Center, Suite 700, 1221 McKinney Street, Houston, TX 770 10, USA
[f] Japan Bioassay Research Center, Japan Industrial Safety and Health Association, 2445 Hirasawa, Hadano, Kanagawa 257-0011, Japan

ARTICLE INFO

Article history:
Received 12 August 2013
Revised 18 September 2013
Accepted 20 September 2013
Available online 30 September 2013

Keywords:
Ethyl *tertiary*-butyl ether
Oxidative stress
8-OHdG
Apoptosis
Liver tumors
Mode of action

ABSTRACT

To elucidate possible mode of action (MOA) and human relevance of hepatotumorigenicity in rats for ethyl *tertiary*-butyl ether (ETBE), male F344 rats were administered ETBE at doses of 0, 150 and 1000 mg/kg body weight twice a day by gavage for 1 and 2 weeks. For comparison, non-genotoxic carcinogen phenobarbital (PB) was applied at a dose of 500 ppm in diet. Significant increase of P450 total content and hydroxyl radical levels by low, high doses of ETBE and PB treatments at weeks 1 and 2, and 8-OHdG formation at week 2, accompanied accumulation of CYP2B1/2B2, CYP3A1/3A2 and CYP2C6, and downregulation of DNA oxoguanine glycosylase 1, induction of apoptosis and cell cycle arrest in hepatocytes, respectively. Up-regulation of CYP2E1 and CYP1A1 at weeks 1 and 2, and peroxisome proliferation at week 2 were found in high dose ETBE group. Results of proteome analysis predicted activation of upstream regulators of gene expression altered by ETBE including constitutive androstane receptor (CAR), pregnane-X-receptor (PXR) and peroxisome proliferator-activated receptors (PPARs). These results indicate that the MOA of ETBE hepatotumorigenicity in rats may be related to induction of oxidative stress, 8-OHdG formation, subsequent cell cycle arrest, and apoptosis, suggesting regenerative cell proliferation after week 2, predominantly via activation of CAR and PXR nuclear receptors by a mechanism similar to that of PB, and differentially by activation of PPARs. The MOA for ETBE hepatotumorigenicity in rats is unlikely to be relevant to humans.

© 2013 Elsevier Inc. All rights reserved.

Introduction

The present study was performed to investigate the mode of action (MOA) of the increased incidence of rat liver tumors for ethyl *tertiary*-butyl ether (ETBE, CAS RN 637-92-3) which is a well-known chemical and gasoline oxygenate synthesized from bioethanol and isobutane. As the use of oxygenated motor fuels is now considered to be beneficial for the environmental consequences due to decrease in exhaust emissions such as carbon monoxide, unburned hydrocarbons, polycyclic aromatics, oxides of nitrogen and particulate carbon, the oil industry of Japan has agreed to use ETBE as a gasoline blending component in order to support the Kyoto Protocol for reducing CO_2 emissions. However, humans are at risk of exposure to oxygenates not only by inhalation while fueling automobiles but also orally when drinking contaminated water (Ahmed, 2001; McGregor, 2006, 2007).

Investigation of ETBE genotoxicity in several test systems including gene mutation tests using Chinese hamster ovary (CHO) cells and *Salmonella typhimurium* strain, chromosomal aberration test with CHO cells, and *in vivo* micronucleus test with bone marrow cells of mice orally treated with ETBE and mice exposed to ETBE by inhalation, showed that ETBE is not genotoxic (ACGIH, 2012; McGregor, 2007).

The information concerning ETBE carcinogenicity in laboratory animals is inconsistent. Previously, increases of total malignant tumors, oncological lesions of the mouth epithelium and forestomach, malignant tumors in the uterus, and haemolymphoreticular neoplasias were observed in a 2-year carcinogenicity study (Maltoni et al., 1999) with Sprague–Dawley rats administered ETBE by stomach tube. However, in another study, ETBE administered for 2-years in drinking water at doses of 0, 625, 2500 or 10,000 ppm was not shown to exert any carcinogenic effects in either male or female F344 rats (Suzuki et al., 2012).

Importantly, ETBE administered to male F344 rats by inhalation at a dose of 5000 ppm for 2-years has been recently shown to induce the development of liver preneoplastic lesions (eosinophilic and basophilic

* Corresponding author. Fax: +81 6 6646 3093.
E-mail address: anna@med.osaka-cu.ac.jp (A. Kakehashi).

0041-008X/$ – see front matter © 2013 Elsevier Inc. All rights reserved.
http://dx.doi.org/10.1016/j.taap.2013.09.016

foci) and hepatocellular adenomas (Saito et al., 2013). Furthermore, in a multi-organ carcinogenesis bioassay, 1000 mg/kg b.w./day ETBE by gavage was found to promote hepatocarcinogenesis in male F344 rats (Hagiwara et al., 2011; Saito et al., 2013). Moreover, in initiation/promotion carcinogenicity assay using N-ethyl-N-(2-hydroxyethyl) nitrosamine (EHEN) as an initiator, the promoting effects of ETBE on hepatocarcinogenesis of male F344 rats were observed at a dose of 1000 mg/kg b.w./day by gavage (Hagiwara, 2012). The MOA of ETBE hepatotumorigenicity in rats is, however, unclear. To elucidate it, we examined production of oxidative stress, alterations to cellular proliferation, apoptosis and identified upstream regulators of differentially expressed genes and proteins in the liver of rats after ETBE administration for 1 and 2 weeks. The effects were compared with those induced by well-known non-genotoxic liver carcinogen, phenobarbital (PB).

Materials and methods

Chemicals

ETBE was manufactured by Nippon Refine Co., Ltd. (Gifu, Japan), and had the following properties: appearance, colorless transparent liquid; boiling point, 70 °C; vapor pressure, 17 kPa (25 °C); solubility, slightly soluble in water (1.2 g/100 g, 20 °C); lot no., L-506251; and purity, >99% (measured by Toray Research Center Co., Ltd., Tokyo, Japan). A single batch of ETBE was used in this study, and the stability was determined by gas chromatography (GC) (Agilent Technologies 5890A, Santa Clara, CA, USA) before the beginning and at the end of the administration period. There were no differences between the results obtained at these two time-points, indicating that the test substance was stable throughout the 2 week examination period.

PB sodium salt (CAS no. 57-30-7) (purity >98%) was purchased from Wako Pure Chemicals Industries (Osaka, Japan). Other reagents were from Wako Pure Chemicals Industries or Sigma (St. Louis, MO).

Animals and treatment

Five-week-old male Fisher F344/DuCrlCrlj rats (Charles River Laboratories Japan Inc. (Tokyo, Japan)) were quarantined for 1 week before the start of the experiments 1 and 2. Animals were housed in an animal facility maintained on a 12 h (8:00–20:00) light/dark cycle, at a constant temperature of 22 ± 3 °C and relative humidity of 55 ± 15% and were given free access to tap water and food (Oriental MF powder diet, Oriental yeast Co., Tokyo, Japan). All experimental procedures were conducted under the Guidelines set by the National Institute of Health and Public Health Service Policy on the Humane Use and Care of Laboratory Animals.

Experimental design

Experiment 1. Before the start of the experiment, eighty male 6-week-old rats were randomized into 4 groups (20 rats/group). ETBE was administered at concentrations of 0 (olive oil-control), 150 (low dose) and 1000 mg/kg body weight (b.w.) (high dose) by intragastrial gavage (i.g.) in the olive oil twice a day with a 6 hour interval for 1 and 2 weeks. PB at a dose of 500 ppm was given to rats for the same periods in MF powder diet. The rats' body weights, water and food intakes were recorded once weekly.

The dose levels and the route of ETBE exposure were selected based on the results of our previous studies where ETBE was found to exert liver tumor promotion effect in rats at a dose of 1000 mg/kg b.w./day, but not 300 mg/kg b.w./day (Hagiwara et al., 2011; Saito et al., 2013). In a preliminary study, F344 rats well tolerated 1000 mg/kg b.w. ETBE administered by gavage twice a day with a 6-hour interval and no abnormalities of general condition were found.

At sacrifice, the liver perfusion was performed through the portal vein as previously described (Kinoshita et al., 2002). The systemic macroscopic pathological examination was performed for all animals. Separate liver portions were fixed in Bouin's solution and 10% buffered formalin. In addition, samples were frozen in liquid nitrogen and stored at −80 °C for biochemical and molecular analyses. Frozen liver tissues (1 g) were processed for microsome isolation (Funae and Imaoka, 1985; Kinoshita et al., 2002).

Experiment 2. The experiment was performed additionally to check the peroxisome proliferation by transmission electron microscopic (TEM) analysis. Twelve male 6-week-old F344 rats were randomized into 4 groups (3 rats/group). ETBE and PB were administered to rats at the same doses as in Experiment 1 for 2 weeks. At sacrifice, livers were removed and processed for histological assessment and subsequent TEM analysis by the standard protocols using 2% glutaraldehyde and 2% paraformaldehyde and 2% osmium tetroxide solutions.

Histopathology

Liver sections (left lateral lobe, median lobe, and right lateral lobe, caudal part) were routinely embedded in paraffin, sectioned, stained with hematoxylin and eosin solution, and examined histopathologically under the light microscope.

ESR

Hydroxyl radicals (OH•) levels in the liver microsomal fraction were detected by electron spin resonance (ESR) technique (Funae and Imaoka, 1985; Kinoshita et al., 2002). The signal intensity of the spin adduct of DMPO and OH• (DMPO–OH) was evaluated from the peak height of the third signal of the quartet and normalized relative to the standard signal intensity of the manganese oxide marker (MnO).

P450 examination

The rat liver microsomal fraction was used for the examination of cytochrome P450 content (Omura and Sato, 1964).

8-hydroxy-2′-deoxyguanosine (8-OHdG) analysis

Extractions of DNAs from the rat liver tissues, and measuring the formation of 8-OHdG by HPLC-ECD were performed by the method of Kasai et al. (1986). Furthermore, liver sections fixed in Bouin's solution were used for 8-OHdG immunohistochemical visualization (Kinoshita et al., 2002).

Real-time quantitative PCR

Total RNA was isolated from rat livers using Isogen (Nippon Gene, Toyama, Japan). Reverse transcription of 3 μg of total RNA was performed with Oligo-dT primer. Real-time quantitative PCR using TaqMan probes and prime sets from TaqMan Gene Expression Assays (4351372) (Applied Biosystems, Japan) was applied for the analysis of mRNA expressions of P450 isoenzymes *Cyp2b1* (Rn01457875_m1), *Cyp2b2* (Rn02786833_m1), *Cyp3a1* (Rn03062228_m1), *Cyp3a2* (Rn00756461_m1), *Cyp2c11* (Rn00569868_m1), *Cyp1a1* (Rn00487218_m1), *Cyp1a2* (Rn00561082_m1), *Cyp2e1* (Rn01759587_m1), *Cyp4a1* (Rn00598510_m1), *Cyp4a2* (Rn00598416_gH) and *Cyp2c6* (TaqMan probe: AGGACA GGAGCCGCATGCCCT; primers Forward-TGATCGTGTGGTTGGCAAA and Reverse-CCTCATGAATCATGGCATCTGT), bile salt sulfotransferase 2 (*Sult2a2*) (Rn02586796_g1), tyrosine-ester sulfotransferase (*Sult1d1*) (Rn00572897_m1), UDP glucuronosyltransferase family 1, polypeptide A1 (*Ugt1a1*) (Rn00754947_m1), UDP glucuronosyltransferase family 2, polypeptide B5 (*Ugt2b5*) (Rn01790037_g1), peroxisome proliferator receptor alpha (*PPARα*) (RN00566193_m1), peroxisome proliferator receptor gamma (*PPARγ*) (RN00440940_m1), oxoguanine glycosylase 1 (*Ogg1*) (Rn01421381_g1), DNA (apurinic or apyrimidinic site) lyase 1

(*APEX1*) (Rn00821186_g1), *p21*$^{WAF1/Cip1}$ (Rn01427989_s1) and cyclin D1 (*CD1*) (TaqMan probe: TCAAGCCTGCGCCAGGCCC; primers: Forward-GCCTGCCAGGAACAGATTGA and Reverse-GGCCTTGGGATCGATGTTCT) (Kakehashi et al., 2009; Kinoshita et al., 2002). Eukaryotic 18S rRNA (4319413E) (Applied biosystems, Japan) was used as an internal control. Results were expressed relative to the number of *18S* RNA transcripts used as an internal control. All measurements were performed in triplicates.

Immunohistochemistry

Staining for PCNA, apoptosis (ssDNA) and P450 isoenzymes (CYPs), was performed by ABC method using mouse monoclonal PCNA (1:500, PC-10, IgG2a; DAKO, Kyoto, Japan), CYP2C6 (1:100, Santa Cruz Biotechnology) and CYP2B1/2 (1:500, Abcam), and rabbit polyclonal ssDNA (1:400, DAKO JAPAN Co., Kyoto, Japan), CYP3A1 (1:1500, Abcam), CYP3A2 (1:500, Abcam), CYP1A1 (1:100, Santa Cruz Biotechnology) and CYP2E1 (1:150x2, Abcam) antibodies. Double immunohistochemistry for 8-OHdG and CYP2B1/2 or CYP3A1 was performed as previously described (Kinoshita et al., 2002). In PCNA and ssDNA staining antigen visualization was done with 3,3′-diaminobenzidine tetrahydrochloride (DAB). At least 6000 hepatocyte nuclei were counted using IPAP in each liver; labeling indices were calculated as the percentage of cell positive for PCNA or ssDNA. P450 staining was assessed qualitatively (Kinoshita et al., 2002).

LC–MS/MS

Reduction, alkylation, digestion and subsequent peptide labeling of 50 μg protein for each sample were performed using the AB Sciex iTRAQ Reagent Multi-Plex Kit as previously described (Gluckmann et al., 2007; Kakehashi et al., 2009). In quantitative analysis, the liver tissues of control, 150 mg/kg b.w. ×2/day ETBE, 1000 mg/kg b.w. ×2/day ETBE and PB groups were labeled with the iTRAQ 114, 115 Da, 116 and 117 signature ion signal reagents, respectively, in MS/MS mode. Proteome analysis was performed on a DiNa-AI nano LC System (KYA Technologies, Tokyo, Japan) coupled to a QSTAR Elite Hybrid mass spectrometer (AB Sciex, Concord, ON, Canada). All reported data were used at 99% confidence cut-off limit. Relative quantitation of peptides was calculated as a ratio by dividing the iTRAQ reporter intensity at 115.0 (low dose ETBE), 116 (high dose ETBE) and 117.0 (PB) m/z by that at 114.0 m/z (control). Protein ratios with a p-value less than 0.05 were considered reliable. In no label analysis, we picked up proteins present (overexpression; not detected in control group), or not present (underexpression; detected in control group) only in livers of rats treated with ETBE and PB.

Ingenuity pathway (IPA) analysis

To assign biological significance to differentially labeled proteins, to identify function and networks of interacting proteins, functional groups and pathways, and prediction of activated up-stream regulators by ETBE and PB, the Ingenuity program (Ingenuity Systems, Mountain View, CA) was utilized. The transcriptional regulation was measured by the z-score. The bases for z-score predictions are relationships in the molecular pathways (networks) which represent experimentally observed protein expression or transcription events. A z-score of above 2 was considered significant.

Statistical analysis

The significance of differences for each parameter (excluding general conditions) was analyzed and evaluated at $P < 0.05$ or $P < 0.01$. Statistical comparisons between the control group and high and low dose ETBE groups of numerical data were conducted using the Bartlett's test. If homogeneous, the data were analyzed with the Dunnett's multiple comparison test (two sided), and if not, with the Steel's test (two sided). Statistical comparisons between control and PB groups, and high dose ETBE and PB groups for numerical data were assessed using the F test. If homogeneous, the data were analyzed with the Student's t-test (two sided), and if not, with the Welch test. The significance of inter group differences in incidences of findings from gross pathology was analyzed using the Fisher's exact probability test (two sided).

Results

Survival and general observations

No animals died throughout the experiment and no abnormalities of general condition were found in any animal of the control, 150, 1000 mg/kg b.w. ×2/day ETBE and 500 ppm PB groups. Mean body weights in low and high dose ETBE groups were comparable to the control. However, those of PB groups were significantly increased at weeks 1 and 2.

No changes of food and water consumptions were observed in ETBE-treated rats, but significant elevation was obvious in PB groups at both time-points. Mean PB intake, calculated from body weights, food consumption, and nominal dietary level, was 39.98 mg/kg b.w./day.

Mean relative liver weights in rats given high dose ETBE (6.10 ± 0.87% and 6.09 ± 0.88%) and PB (6.77 ± 0.75% and 6.00 ± 0.71%) were significantly higher as compared to controls (4.88 ± 0.50% and 4.65 ± 0.56%) at both weeks 1 and 2.

Macroscopic pathology

No treatment-related macroscopic changes except for the liver were found in the low, high dose ETBE and PB-treated rats. Although color of the liver in control rats was pale brown, those in high dose ETBE and PB groups were pale red and appeared swollen at both weeks 1 and 2 (Fig. 1A). The representative photographs were taken at week 2.

Liver histopathology

At week 1, slight hepatocellular hypertrophy was observed at incidences of 10% and 70% in low and high dose ETBE groups, respectively. At week 2, slight and moderate hypertrophy (60%) was detected in high dose ETBE group. Moderate hepatocellular hypertrophy was found in all rats fed PB at both weeks. Observed hepatocellular hypertrophy was centrilobular (Fig. 1A).

Hydroxyl radical generation

As shown in Table 1, significant elevation of OH• levels in the liver tissues of high dose ETBE and PB-treated rats, was found at weeks 1 and 2 (Table 1). In the high dose ETBE group they were significantly lower than that of PB-administered rats.

P450 total content

Spectrophotometric analysis of liver microsomes revealed significant increases of P450 content levels in the liver of high dose ETBE and PB-treated animals as compared to the controls at both experimental weeks (Table 1). Slight, but significant increase was also noted in low dose ETBE group at week 1, but not week 2. In the livers of high dose ETBE-treated animals, P450 induction was lower than in PB group, but without significance.

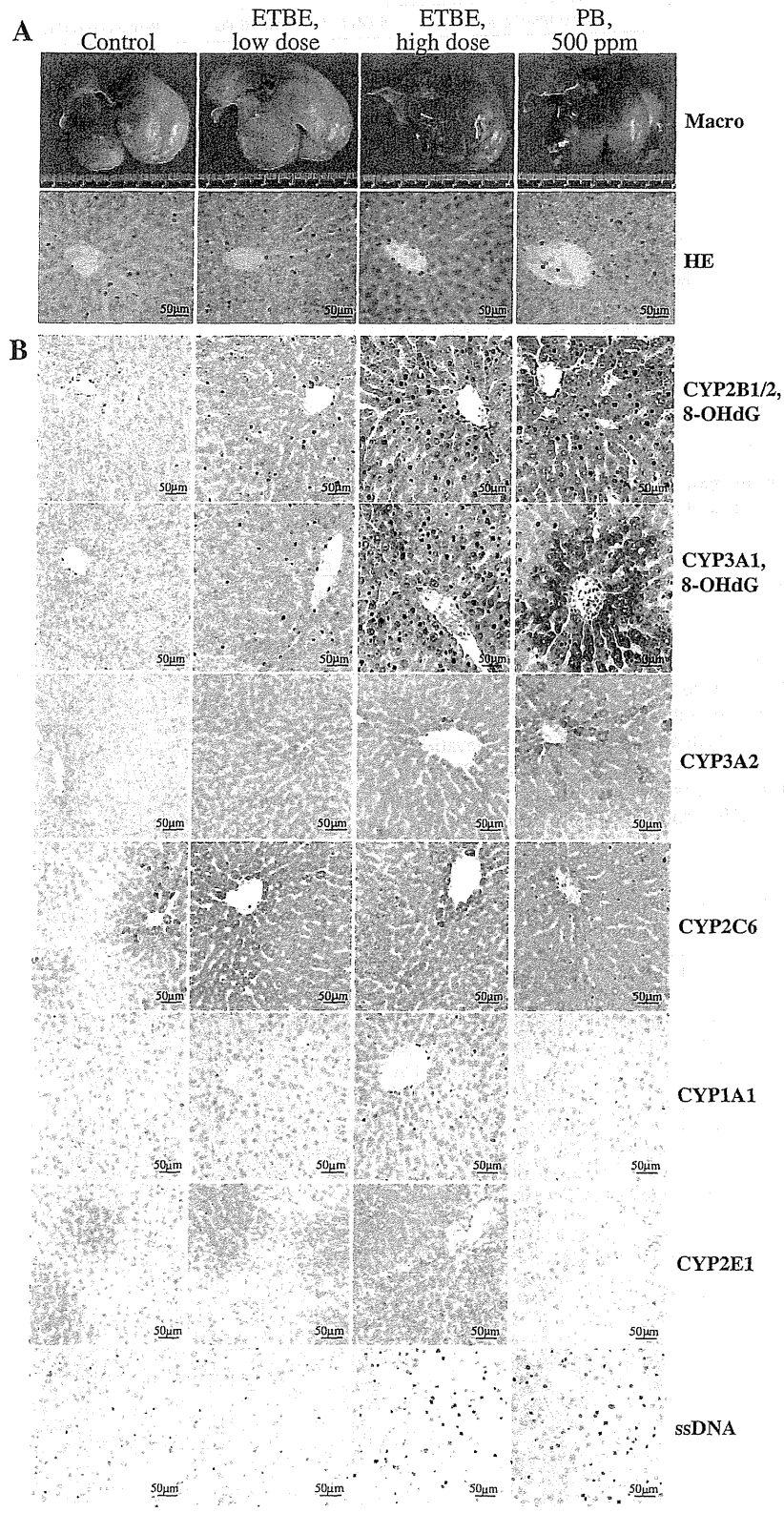

Fig. 1. Macroscopic and histopathological examinations (week 2) (A) and immunohistochemical analyses (week 2) (B): double immunohistochemistry for CYP2B1/2, CYP3A1 and 8-OHdG, immunohistochemistry for CYP3A2, CYP2C6, CYP1A1, CYP2E1, and detection of apoptosis (ssDNA) in the livers of rats treated with ETBE and PB. Note the pale red color of high dose ETBE and PB-treated rat livers. In double staining, the red color cytoplasm of hepatocytes reflects binding of rabbit polyclonal primary antibody against cytochrome P450, while brown or black stained nuclei showed positive immunoreactions for monoclonal primary antibody against 8-OHdG. Note the increase of 8-OHdG in the nuclei of pericentrally localized hepatocytes most strongly stained for CYP2B1/2 and CYP3A1. Similar to 8-OHdG, nuclei of pericentrally localized hepatocytes were also positive for ssDNA.

Table 1
Induction of oxidative stress, peroxisome proliferation and alteration to cell proliferation and apoptosis in the liver of rats induced by ETBE and PB.

Group	OH• radicals (RI (%))	P450 (nmol/mg protein)	8-OHdG (8-OHdG/10^5dG)	Peroxisomes (No./cell)	PCNA (%)	ssDNA (%)
Week 1						
Control	83.4 ± 11.5	649.1 ± 129.3	0.250 ± 0.031	NE	6.13 ± 1.59	1.15 ± 0.60
ETBE, low dose	91.1 ± 15.3	1078.0 ± 471.2[a]	0.220 ± 0.034	NE	7.11 ± 2.23	1.38 ± 1.04
ETBE, high dose	117.8 ± 17.1[b,*]	1887.2 ± 513.8[c]	0.259 ± 0.044	NE	8.06 ± 1.98	1.76 ± 1.99
PB, 500 ppm	176.5 ± 27.5[b]	2474.7 ± 808.2[c]	0.232 ± 0.040	NE	16.49 ± 3.97[b]	1.17 ± 0.87
Week 2						
Control	65.1 ± 11.8	847.3 ± 302.9	0.257 ± 0.025	6.25 ± 1.15	6.22 ± 0.60	0.97 ± 0.41
ETBE, low dose	70.4 ± 12.1	933.5 ± 314.6	0.258 ± 0.069	14.33 ± 1.38[b]	5.48 ± 1.33	0.99 ± 0.26
ETBE, high dose	95.2 ± 22.7[a,*]	1839.9 ± 555.6[b]	0.356 ± 0.047[a]	35.67 ± 2.08[c]	2.94 ± 0.75[b]	8.58 ± 5.42[a]
PB, 500 ppm	152.8 ± 29.0[b]	2218.0 ± 826.4[b]	0.366 ± 0.056[a]	7.00 ± 0.90	3.07 ± 0.46[b]	7.53 ± 3.72[a]

Data are Mean ± SD; NE, not examined; low dose, 150 mg/kg b.w. ×2/day; high dose, 1000 mg/kg b.w. ×2/day.
[a] $P < 0.05$ *vs* control group.
[b] $P < 0.01$ *vs* control group.
[c] $P < 0.0001$ *vs* control group.
* $P < 0.01$ *vs* PB group.

8-OHdG (HPLC-ECD)

Comparable significant increases of 8-OHdG levels in rat liver DNA were found in high dose ETBE and PB groups as compared to the controls at week 2 (Table 1).

Changes to mRNA expression of P450 isoenzymes and other CAR, PXR and PPARs-responsive elements

In line with P450 content and OH• levels, significant overexpressions of *Cyp2b1*, *Cyp2b2* and *Cyp3a1* mRNA were found in high dose ETBE and PB groups as compared to control rats at weeks 1 and 2 (Table 2). Furthermore, the tendency for increase and significant elevation of *Cyp3a2* mRNA levels was observed in high dose ETBE and PB-treated rats, respectively. Significant increases of *Cyp2b1* and *Cyp2b2* mRNA were apparent in low dose ETBE group at week 1 but not week 2. In the livers of high dose ETBE-administered rats, *Cyp2b1* (weeks 1 and 2), *Cyp2b2* (weeks 1 and 2) and *Cyp3a1* (week 2) mRNA levels were significantly lower than that of PB group. *Cyp2c11* mRNA was significantly elevated only in PB-treated rats at both time-points (Table 2).

Ugt1a1 mRNA expression was significantly inhibited in high dose ETBE and PB groups at week 2 (Table 2). On the contrary, significant overexpression of *Ugt2b5* mRNA was apparent in those groups at week 1.

Significant suppression of *Sult1d1* mRNA expression was detected in high dose ETBE (week 1) and PB (weeks 1 and 2) groups (Table 2). Its levels were elevated in high dose ETBE group as compared to PB group with significant difference observed at week 2. Furthermore, significant downregulation of *Sult2a2* mRNA was found in PB-administered rats at weeks 1 and 2.

Specific significant overexpression of *Cyp1a1* and *CYP2e1* mRNA was detected only in high dose ETBE-administered rats at weeks 1 and 2,

Table 2
Alterations to mRNA expression of genes associated with of formation of oxidative stress, DNA repair and cell cycle arrest induced by ETBE and PB.

Gene	Week 1				Week 2			
	Control	ETBE, low dose	ETBE, high dose	PB, 500 ppm	Control	ETBE, low dose	ETBE, high dose	PB, 500 ppm
Cyp2b1	0.01 ± 0.00	0.014 ± 0.00[b]	0.09 ± 0.03[c,¶]	0.48 ± 0.16[c]	0.01 ± 0.00	0.01 ± 0.00	0.07 ± 0.03[c,¶]	0.43 ± 0.07[c]
Cyp2b2	0.07 ± 0.02	0.09 ± 0.02[a]	0.34 ± 0.10[c,¶]	1.01 ± 0.37[c]	0.06 ± 0.02	0.07 ± 0.02	0.24 ± 0.10[c,¶]	0.98 ± 0.32[c]
Cyp3a1	0.38 ± 0.11	0.41 ± 0.14	1.08 ± 0.49[c]	1.39 ± 0.45[b]	0.30 ± 0.15	0.24 ± 0.08	0.59 ± 0.15[c,§]	0.91 ± 0.21[d]
Cyp3a2	0.94 ± 0.23	0.99 ± 0.27	1.29 ± 0.47	1.64 ± 0.47[b]	0.73 ± 0.19	0.68 ± 0.10	0.90 ± 0.31	1.17 ± 0.29[b]
Ugt1a1	0.12 ± 0.03	0.12 ± 0.03	0.12 ± 0.03	0.09 ± 0.03	0.15 ± 0.05	0.11 ± 0.03	0.11 ± 0.03[a]	0.10 ± 0.05[a]
Ugt2b5	0.21 ± 0.04	0.23 ± 0.05	0.31 ± 0.12[a]	0.35 ± 0.10[b]	0.32 ± 0.04	0.31 ± 0.05	0.32 ± 0.07	0.35 ± 0.09
Sult1d1	0.79 ± 0.17	0.72 ± 0.23	0.55 ± 0.22[a]	0.48 ± 0.12[b]	1.17 ± 0.55	0.82 ± 0.16	0.81 ± 0.30[*]	0.56 ± 0.20[b]
Sult2a2	0.45 ± 0.25	0.37 ± 0.14	0.42 ± 0.13[§]	0.18 ± 0.07[b]	0.42 ± 0.16	0.39 ± 0.24	0.37 ± 0.16[§]	0.10 ± 0.06[c]
Cyp2c11	0.24 ± 0.05	0.27 ± 0.04	0.25 ± 0.06[¶]	0.43 ± 0.07[d]	0.25 ± 0.06	0.25 ± 0.04	0.27 ± 0.07[¶]	0.57 ± 0.09[d]
Cyp1a1	0.11 ± 0.03	0.11 ± 0.05	0.38 ± 0.14[c,§]	0.16 ± 0.10	0.12 ± 0.04	0.10 ± 0.03	0.28 ± 0.11[b,#]	0.10 ± 0.09
Cyp1a2	2.47 ± 0.61	2.47 ± 0.46	2.30 ± 0.88[#]	0.74 ± 0.20[c]	1.78 ± 0.57	1.59 ± 0.24	1.80 ± 0.56[¶]	0.64 ± 0.20[c]
Cyp2c6	0.06 ± 0.01	0.08 ± 0.02[a]	0.15 ± 0.06[c]	0.21 ± 0.08[c]	0.07 ± 0.01	0.09 ± 0.02[b]	0.15 ± 0.03[c,§]	0.22 ± 0.05[c]
Cyp2e1	1.51 ± 0.40	1.47 ± 0.37	2.22 ± 1.00[a,*]	1.21 ± 0.28	1.53 ± 0.26	1.63 ± 0.25	1.95 ± 0.25[a]	1.22 ± 0.15
Cyp4a1	3.02 ± 0.74	3.36 ± 1.41	3.66 ± 2.74[*]	1.34 ± 0.44[b]	5.36 ± 1.13	5.58 ± 1.17	5.38 ± 1.88[*]	1.35 ± 0.36
Cyp4a2	2.00 ± 0.49	2.17 ± 0.54	2.24 ± 1.06[§]	0.97 ± 0.29[b]	2.71 ± 0.41	2.99 ± 0.40	2.93 ± 0.96[§]	1.17 ± 0.19[b]
PPARα	1.21 ± 0.36	1.70 ± 0.89	2.23 ± 1.32[a]	1.42 ± 0.49	1.69 ± 0.36	1.73 ± 0.54	1.74 ± 0.36[*]	1.26 ± 0.10
PPARγ	0.47 ± 0.20	0.63 ± 0.19	0.84 ± 0.31[a]	1.41 ± 0.77[a]	0.89 ± 0.59	1.09 ± 0.61	1.54 ± 0.80[*]	3.11 ± 1.52[b]
Ogg1	0.43 ± 0.06	0.39 ± 0.09	0.34 ± 0.15	0.33 ± 0.05[b]	0.45 ± 0.08	0.42 ± 0.09	0.36 ± 0.08	0.31 ± 0.10[b]
APEX1	0.66 ± 0.05	0.71 ± 0.10	0.76 ± 0.18[*]	0.58 ± 0.07	0.78 ± 0.14	0.79 ± 0.14	0.84 ± 0.16[#]	0.57 ± 0.11[b]
CD1	0.30 ± 0.10	0.29 ± 0.09	0.28 ± 0.12	0.35 ± 0.11	0.25 ± 0.05	0.24 ± 0.03	0.18 ± 0.03[b]	0.22 ± 0.08
p21$^{WAF1/Cip1}$	0.46 ± 0.16	0.45 ± 0.21	0.42 ± 0.19	0.36 ± 0.06	0.51 ± 0.15	0.52 ± 0.19	0.40 ± 0.09	0.34 ± 0.08[a]

Data are Mean ± SD; Gene/18rRNA; low dose, 150 mg/kg b.w. ×2/day; high dose, 1000 mg/kg b.w. ×2/day.
[a] $P < 0.05$ *vs* control group.
[b] $P < 0.01$ *vs* control group.
[c] $P < 0.001$ *vs* control group.
[d] $P < 0.0001$ *vs* control group.
* $P < 0.05$ *vs* 500 ppm PB group.
§ $P < 0.01$ *vs* 500 ppm PB group.
# $P < 0.001$ *vs* 500 ppm PB group.
¶ $P < 0.0001$ *vs* 500 ppm PB group.

being significantly higher than in PB-treated rats (Table 2). *Cyp1a2* mRNA expression was significantly decreased only in PB group at examined time-points.

Significant elevation of *Cyp2c6* mRNA expression was observed in rats given low and high dose ETBE and PB at both weeks (Table 2). Its values were lower in high dose ETBE group as compared to PB-treated rats with significant difference at week 2.

PPARα-related *Cyp4a1* and *Cyp4a2* mRNA levels tended for increase in high dose ETBE group at week 1 but returned to normal levels at week 2 (Table 2). In PB-treated rats significant downregulation was observed at both experimental weeks.

In line with *Cyp4a1/2* mRNA changes, *PPARα* mRNA level was significantly elevated as compared to the control only in high dose ETBE group at week 1 being higher than that of PB group (Table 2), but returned to level comparable to normal at week 2. Furthermore, significant *PPARγ* upregulation was obvious in both high dose ETBE (week 1) and PB (weeks 1 and 2) groups.

Alterations to mRNA expression of DNA repair enzymes

Tendency for decrease and significant inhibition of *Ogg1* mRNA expression were observed in high dose ETBE and PB-treated rat livers, respectively, at both weeks 1 and 2 (Table 2). No significant changes of *APEX1* mRNA levels were detected in ETBE groups, but a tendency for decrease and significant inhibition of *APEX1* mRNA levels were noted in PB-treated rats at weeks 1 and 2, respectively.

CD1 and $p21^{WAF1/Cip1}$

No significant differences in *CD1* mRNA expression were observed at week 1, while the significant inhibition and a tendency for decrease were noted in high dose ETBE and PB groups, respectively, at week 2 (Table 2).

A trend for decrease of $p21^{WAF1/Cip1}$ mRNA was observed in high dose ETBE group at week 2 (Table 2). Furthermore, in PB-treated rats, a tendency for decrease and significant inhibition were detected at weeks 1 and 2, respectively.

Immunohistochemical findings

In high dose ETBE and PB-treated rat livers, the strongest overexpression (intense staining) mostly in the centrilobular hepatocellular regions was observed for CYP2B1/2 as compared to the control rats at weeks 1 and 2 (Fig. 1B). Moderate overexpression was found for CYP3A1, CYP3A2 (week 2) and CYP2C6 (week 2) in both groups. More pronounced elevations of those isoenzymes were obvious in PB-treated rats.

In high dose ETBE group, moderate and slight overexpression of CYP2E1 (weeks 1 and 2) and CYP1A1 (week 1), respectively, was found (Fig. 1B). However, no elevation of CYP2E1 and CYP1A1 protein expression was detected in PB-treated rats.

Double immunohistochemistry demonstrated intense centrilobular cytoplasmic CYP2B1/2B2 and CYP3A1 immunoreactivity, and apparent increased numbers of intensely 8-OHdG immunolabeled nuclei in the centrilobular liver region in high dose ETBE and PB groups at week 2 (Fig. 1B). Slight staining for CYP2B1/2B2, CYP3A1 and 8-OHdG was also observed in low dose ETBE-treated rats at week 2. Hepatocytes most strongly positive for those CYPs were also positive for 8-OHdG. Intensity of CYP2B1/2 and CYP3A1 staining in high dose ETBE-treated rat livers was lower than that of PB-administered rats but the intensity of 8-OHdG staining was comparable in both groups.

Alterations to cell proliferation (PCNA)

The trend for increase and significant elevation of PCNA positive cell ratio for hepatocytes were observed in high dose ETBE and PB-treated rats, respectively, at week 1 (Table 1). On the contrary, significant inhibition of PCNA indices in high dose ETBE and PB groups was obvious at week 2. PCNA indices in the control and low dose ETBE groups were comparable at both time-points.

Evaluation of apoptosis (ssDNA)

As shown in Table 1, significant 8 and 7-fold increases in the number of apoptotic cells were found at week 2, but not week 1, following high dose ETBE and PB administration, respectively. No induction of apoptosis was observed in low dose ETBE group. Only nuclei of hepatocytes localized in the centrilobular region were positively stained for ssDNA (Fig. 1B). Correlations were clearly apparent with alterations in 8-OHdG (Table 1 and Fig. 1B).

Alterations to protein expression in rat livers and IPA analysis

In iTRAQ quantitative analysis, at week 1, significant elevation of expression of 86, 103 and 92 proteins and suppression of 70, 72 and 82 proteins in low dose ETBE, high dose ETBE and PB groups, respectively, were detected. At week 2, significant increase of expression of 34, 79 and 102 proteins and inhibition of 39, 83 and 91 proteins in low dose ETBE, high dose ETBE and PB groups, respectively, were found. In no label analysis, significant elevation of expression of 114, 102 and 68 proteins and suppression of 12, 21 and 20 proteins in low dose ETBE, high dose ETBE and PB groups, respectively, were detected at week 1. Furthermore, significant elevation of 82, 119 and 83 proteins and underexpression of 22, 20 and 29 proteins in low dose ETBE, high dose ETBE and PB groups, respectively, were detected at week 2. The spectrum of changes appeared to be similar in high dose ETBE and PB-administered rat livers.

Comparison analysis of protein functions by IPA indicated that treatment with ETBE mostly altered the number and expression of proteins involved in energy production, lipid and fatty acid metabolism, small molecule biochemistry and cell death. In PB-treated rats, proteins which participated in drug, amino acid and nucleic acid metabolism showed higher elevation. Significant alteration to fatty acid, tryptophan, linoleic acid metabolisms and bile acid biosynthesis was observed in high dose ETBE-treated rat livers at week 2. Numbers of overexpressed proteins participated in regulation of LPS/IL-1-mediated inhibition of RXR function, metabolism of xenobiotics by cytochrome P450, Nrf-2-mediated oxidative stress response and PXR/RXR activation were increased in high dose ETBE and PB-treated rats mostly at week 2 and those changes were more pronounced in PB group.

Several differentially expressed proteins in the rat livers influenced by high dose ETBE and PB treatments are presented in Table 3. Similar significant elevations of xenobiotic metabolism enzymes CYP2B1/2B2, CYP3A1/3A2, CYP2C6, CYP2C55, CYP2A2, glutathione *S*-transferase (GST) alpha 1 (GSTA1), alpha 3 (GSTA3) and alpha 5 (GSTA5), GST mu 5 (GSTM5), glutathione peroxidase 1 (GPX1), epoxide hydrolase 1, microsomal (EPHX1), carboxylesterase 3 (CES3), cytochrome P450 oxidoreductase (POR), UGT2B1, UGT2B5 and UDP-glucose 6-dehydrogenase (UGDH) in both groups were demonstrated.

The specific changes in high dose ETBE-treated rat livers included elevations of acyl-CoA oxidase 1, palmitoyl (ACOX1), enoyl CoA hydratase 1, peroxisomal (ECH1), solute carrier family 27, member 2 (SLC27A2), solute carrier family 27, member 5 (SLC27A5) and CYP4A2 participated in fatty acid metabolism, and CYP2E1, CYP2G1, ferredoxin 1 (FDX1), superoxide dismutase 2, mitochondrial (SOD2), retinol binding protein 4, plasma (RBP4) and ubiquinol-cytochrome c reductase core protein I (UQCRC1) were involved in xenobiotic metabolism. Overexpression of CYP1A1 was not detected by proteome analysis, but observed at week 2 by the immunohistochemical examination (Fig. 1B).

CYP2C11, CYP2C12, and UDP glucuronosyltransferase 1 family, polypeptide A6 (UGT1A6) were specifically overexpressed only in PB-treated rats.

Table 3
Differentially expressed proteins in the liver of rats treated with high dose ETBE and 500 ppm PB, identified by QSTAR LC–MS/MS.

Protein	GI number	Location	Type	Function	Week 1				Week 2			
					ETBE		PB		ETBE		PB	
					Ratio	P	Ratio	P	Ratio	P	Ratio	P
Aldehyde dehydrogenase 1 family, member A1 (ALDH1A1)	14424442	C	E	AM	1.20	0.0007	1.90	0.0000	1.48	0.0009	1.96	0.0000
Arginase, liver (ARG1)	114146	C	E	AAM, A	1.20	0.0218	–	–	1.21	0.0302	1.40	0.0000
Argininosuccinate synthase 1 (ASS1)	114291	C	E	AAM,	–	–	–	–	1.20	0.0012	1.44	0.0000
Ketohexokinase (fructokinase) (KHK)	400132	C	K	CM	–	–	–	–	↑	0.0000	–	–
Pyruvate dehydrogenase kinase, isozyme 2 (PDK2)	3183110	C	K	CM	–	–	–	–	↑	0.0000	–	–
Phosphogluconate dehydrogenase (PGD)	205686170	C	E	CM	–	–	–	–	1.25	0.0115	–	–
Purine nucleoside phosphorylase (PNP)	205829287	C,ES,N	E	PNM,AP	–	–	–	–	↑	0.0000	–	–
Acyl-CoA oxidase 1, palmitoyl (ACOX1)	115565	C,Mi,P	E	LM	0.82	0.0011	0.83	0.0019	2.18	0.0000	–	–
Enoyl CoA hydratase 1, peroxisomal (ECH1)	6015047	C,Mi,P	E	LM	–	–	0.64	0.0000	1.47	0.0136	0.67	0.0000
Paraoxonase 1 (PON1)	2829441	ES	Ph	LM	–	–	2.4	0.0000	1.72	0.0001	2.63	0.0000
Apolipoprotein E (APOE)	1703338	ES,C	T	LM	–	–	–	–	↑	0.0000	↑	0.0000
Solute carrier family 27, member 2 (SLC27A2)	3183199	C,P,Mi	T	LM	–	–	–	–	2.12	0.0000	–	–
Solute carrier family 27, member 5 (SLC27A5)	81906294	C	T	LM	–	–	–	–	1.23	0.0060	–	–
Epoxide hydrolase 1, microsomal (xenobiotic) (EPHX1)	123928	C,EPR	Pe	XM,LM	1.40	0.0000	2.54	0.0000	1.51	0.0001	2.52	0.0000
Carboxylesterase 3 (CES3)	57013350	C,EPR	E	XM,LM	1.21	0.0009	1.34	0.0000	1.33	0.0015	1.36	0.0002
Cytochrome P450, family 2, subfam. a, polypept. 2 (CYP2A2)	117193	C	E	XM,LM	–	–	–	–	1.40	0.0027	1.66	0.0018
Cytochrome P450, family 2, subfam. b, polypept. 1 (CYP2B1)	117206	C,EPR	E	XM	2.19	0.0000	4.25	0.0000	2.92	0.0076	5.49	0.0024
Cytochrome P450, family 2, subfam. b, polypept. 2 (CYP2B2)	3123191	C,EPR	E	XM,OR	↑	0.0000	↑	0.0000	1.65	0.0035	2.53	0.0008
Cytochrome P450, family 2, subfam. b, polypept. 3 (CYP2B3)	117210	C,EPR	E	XM,OR	↑	0.0000	–	–	–	–	–	–
Cytochrome P450, family 2, subfam. c, polypept. 6 (CYP2C6)	117223	C,EPR,Mi	E	XM,OR	–	–	2.35	0.0000	1.51	0.0014	2.8	0.0000
Cytochrome P450, family 2, subfam. c, polypept. 55 (CYP2C55)	143811382	C,EPR	E	XM,OR	–	–	–	–	↑	0.0000	↑	0.0000
Cytochrome P450, family 2, subfam. c, polypept. 11 (CYP2C11)	117228	C,EPR	E	XM,OR	0.72	0.0011	1.20	0.0015	–	–	1.69	0.0000
Cytochrome P450, family 2, subfam. c, polypept. 12 (CYP2C12)	117229	C,EPR	E	XM,OR	–	–	–	–	–	–	↑	0.0000
Cytochrome P450, fam. 2, subfam. E, polypept. 1 (CYP2E1)	1352193	C,EPR,Mi	E	XM,OR	↑	0.0000	–	–	↑	0.0000	–	–
Cytochrome P450, fam. 2, subfam. G, polypept. 1 (CYP2G1)	117255	C,EPR	E	XM,OR	–	–	–	–	↑	0.0000	–	–
Cytochrome P450, fam. 3, subfam. A, polypept. 1 (CYP3A1)	148540156	C,EPR	E	XM,OR	–	–	3.70	0.0000	1.54	0.0000	2.86	0.0004
Cytochrome P450, fam. 3, subfam. A, polypept. 2 (CYP3A2)	6166033	C,EPR	E	XM,OR	–	–	3.24	0.0000	1.33	0.0000	2.48	0.0003
Cytochrome P450, fam. 4, subfam. A, polypept. 2 (CYP4A2)	117164	C,EPR	E	XM,OR	↑	0.0000	–	–	↑	0.0000	–	–
Glutathione S-transferase alpha 1 (GSTA1)	1170084	C,N	E	XM,GM	1.42	0.0000	1.25	0.0000	1.21	0.0001	1.20	0.0005
Glutathione S-transferase alpha 3 (GSTA3)	1170085	C	E	XM,GM	–	–	–	–	5.81	0.0001	5.39	0.0005
Glutathione S-transferase alpha 5 (GSTA5)	121713	C,N	E	XM,GM	1.61	0.0000	3.03	0.0000	1.78	0.0000	3.24	0.0000
Glutathione S-transferase mu 5 (GSTM5)	121717	C,EPR	E	XM,GM	1.18	0.0000	1.58	0.0000	1.68	0.0000	2.37	0.0000
UDP glucuronosyltransferase 1 fam., polypept. A1 (UGT1A1)	2501473	C,EPR	E	XM,LM	–	–	–	–	↓	0.0000	↓	0.0000
UDP glucuronosyltransferase 1 fam., polypept. A3 (UGT1A3)	2501475	C,EPR	E	XM	↑	0.0000	–	–	–	–	–	–
UDP glucuronosyltransferase 1 fam., polypept. A6 (UGT1A6)	136726	C,EPR,Mi	E	XM	–	–	–	–	–	–	1.42	0.0016
UDP glucuronosyltransferase 2 fam., polypept. B1 (UGT2B1)	136728	C,EPR	E	XM	1.58	0.0008	2.97	0.000	1.46	0.0005	2.3	0.0000
UDP glucuronosyltransferase 2 fam., polypept. B5 (UGT2B5)	136730	C,EPR,Mi	E	XM	↑	0.0000	↑	0.000	↑	0.0000	↑	0.0000
P450 (cytochrome) oxidoreductase (POR)	127966	C,EPR,Mi	E	XM,OR	–	–	1.27	0.0000	1.73	0.0000	2.09	0.0000
UDP-glucose 6-dehydrogenase (UGDH)	6136118	C,N	E	XM,OR	1.35	0.0116	–	–	1.51	0.0006	1.26	0.0037
Glutathione peroxidase 1 (GPX1)	172046776	C	E	ReOS,GM	2.18	0.0000	1.20	0.0000	1.64	0.0000	1.70	0.0000
Ferredoxin 1 (FDX1)	113473	C,Mi	T	XM,ET	–	–	–	–	↑	0.0000	–	–
Superoxide dismutase 1, soluble (SOD1)	134625	C,Mi,P	E	XM,ReE	1.75	0.0000	0.78	0.0000	0.55	0.0000	0.65	0.0000
Superoxide dismutase 2, mitochondrial (SOD2)	134678	C,Mi,P	E	ReOS,ReE	–	–	–	–	↑	0.0000	–	–
Retinol binding protein 4, plasma (RBP4)	132407	ES,C	T	ReE	2.15	0.0000	–	–	1.27	0.0009	–	–
Ubiquinol-cytochrome c reductase core protein I (UQCRC1)	81884378	C,Mi	E	ReA,OR	–	–	–	–	↑	0.0000	–	–
Cytochrome b5 type A (microsomal) (CYB5A)	231928	C	E	ET	1.27	0.0000	1.97	0.0000	–	–	1.43	0.0000
Cytochrome c oxidase subunit Vb (COX5B)	1352167	C,Mi	E	ET	1.50	0.0000	1.20	0.0029	0.48	0.0000	0.49	0.0000
Electron-transferring-flavoprotein dehydrogenase (ETFDH)	52000614	C,Mi	E	ET,ReOS	0.86	0.0145	0.80	0.0001	1.20	0.0263	–	–
Collagen, type I, alpha 2 (COL1A2)	19855071	ES	O	FO	4.35	0.0000	1.26	0.0005	1.27	0.0000	9.27	0.0000
Keratin 18 (KRT18)	73621121	C	O	CO,ST	0.92	0.0053	0.87	0.0041	–	–	–	–
Keratin 8 (KRT8)	1708592	C	O	CO,ST	0.93	0.0422	–		–	–	–	–
Actinin, alpha 1 (ACTN1)	13123942	C	O	CO	–		–	–	↑	0.0000	–	–
Plectin (PLEC)	1709655	PM,C	O	CO,AP	↑	0.0000	–	–	↑	0.0000	–	–
Myristoylated alanine-rich protein kinase C substrate (MARCKS)	266495	PM,C	O	CO	↑	0.0000	↑	0.0000	↑	0.0000	↑	0.0000
MAP/microtubule affinity-regulating kinase 3 (MARK3)	81170677	PM	K	ST	–		–	–	↑	0.0000	–	–
Inositol 1,4,5-trisphosphate receptor, type 1 (ITPR1)	17380349	C,EPR,G	IC	ST,	–	–	–	–	↑	0.0000	–	–
Mechanistic target of rapamycin (MTOR)	1169736	C,EPR,G	K	ST,CO	–	–	–	–	↑	0.0000	–	–
RAB3A interacting protein (rabin3) (RAB3IP)	71152027	C,N	O	PT	–	–	–	–	↑	0.0000	–	–
Protein disulfide isomerase family A, member 6 (PDIA6)	62296810	C,EPR	E	PF	1.26	0.0142	3.3	0.0000	4.01	0.0000	1.24	0.0028
Heat shock protein 90 kDa alpha, class A member 1 (HSP90AA1)	122065208	C,Mi	E	PF	–	–	–	–	1.24	0.0375	1.27	0.0114
Heat shock 70 kDa protein 2 (HSPA2)	148887381	C,Mi,N	O	PF	3.31	0.0000	–	–	1.22	0.0250	1.32	0.0414
Calnexin (CANX)	543922	C,EPR	O	PF,A	–		–	–	0.77	0.0073	–	–

1. C: cytoplasm; ES: extracellular space; EPR: endoplasmic reticulum; G: Golgi apparatus; Mi: mitochondria; N: nucleus; P: peroxisome; PM: plasma membrane.
2. E: enzyme; IC, ion channel; K: kinase; Pe: peptidase; Ph: phosphatase; T: transporter; O: other.
3. A: aging; AAM: amino acid metabolism; AM: alcohol metabolism; AP: apoptotic process; CM: cellular metabolism; CO: cytoskeleton organization; ET: electron transport; FO: fibril organization; GM: glutathione metabolism; LM: lipid metabolism; PF: protein folding; PNM: purine nucleoside metabolism; PT: protein transport; OR: oxidation–reduction process; ReA, response to alkaloid; ReE: response to ethanol; ReOS: response to oxidative stress; ST, signal transduction; XM: xenobiotic metabolism, ↑: up-regulation (no expression detected in the control group) and ↓: down-regulation (no expression detected in treatment group) in no label proteome analysis; –: no change; Ratio: ratio to control group.

Comparison of activated up-stream regulators by IPA

Activation of CAR and PXR nuclear receptors by both high dose of ETBE (z-score: 2.130 (CAR); 2.000 (PXR)) and PB (z-score: 3.167 (CAR); 3.061 (PXR)) was predicted by IPA at week 2 (Fig. 2). This activation was accompanied by predicted concomitant activation of NF-kB, HNF4A, ARNT2 and SIM1 transcriptional factors. PB treatment induced CAR and PXR activation as early as week 1 of application, thus, indicating that PB is a stronger inducer than ETBE. Activation of arylhydrocarbon nuclear receptor (AhR) was not predicted by IPA.

Interestingly, in high dose ETBE-treated rat livers, activation of PPARγ (z-score: 2.082) and PPARδ (z-score: 2.100) nuclear receptors, and a possibility of activation of PPARα (z-score: 1.282; P value: 6.96E-33) were predicted by IPA dependent of up-regulation of CYP4A2, ACOX1, ECH1, SLC27A2, SLC27A5, and other enzymes involved in fatty acid metabolism in mitochondria. These changes were suggested to be associated with activation of TFAM transcription factor. We further decided to check the possibility of PPARα activation in terms of peroxisome proliferation by ETBE using transmission electron microscopy (TEM) analysis.

TEM

Representative TEM findings in hepatocytes of F344 rats given ETBE or PB for 2 weeks are shown in Fig. 3. Average number of peroxisomes in hepatocytes was markedly elevated in high dose ETBE group (Table 1). It was also increased slightly, but significantly, in low dose ETBE-treated rats. However, in PB-administered animals the average number of peroxisomes was comparable to the control level.

Discussion

The present study demonstrated that short-term exposure to non-genotoxic chemical, ETBE administered to rats by gavage activated CAR and PXR nuclear receptors in the livers similar to the mechanism possessed by non-genotoxic chemical carcinogen PB, and furthermore specifically activated PPARs, thus, leading to conspicuous elevation of 8-OHdG formation, cell cycle arrest and apoptosis due to the development of oxidative stress, activation of fatty acid metabolism in mitochondria and peroxisome proliferation in hepatocytes.

Three possible MOA for the hepatocellular tumor induction in laboratory animals are suggested to include direct DNA reactivity, enzyme induction/enhanced cell proliferation in preneoplastic foci/tumor development and cytotoxicity followed by regenerative cell proliferation (Fenner-Crisp et al., 2011). The postulated MOA underlying the etiology of rodent liver tumors is exhibited by the non-genotoxic chemical carcinogen PB which could be used for comparison. According to the results of the present investigation and our previous study on ETBE tumorigenicity (Saito et al., 2013), PB MOA appeared to be similar to that of high dose ETBE except the PPAR activation. Activation of CAR and PXR by both chemicals caused up-regulation of numerous downstream proteins such as CYP2B1 and 2B2, CYP3A1 and 3A2, Ugt2b5 and others, which resulted in significant elevation of total P450 content, generation of hydroxyl radicals, 8-OHdG formation and lastly induction of cell cycle arrest and apoptosis in the rat livers after 2 weeks of application (Fig. 4). Observed inhibition of *CD1* and $p21^{WA1Cip1}$ mRNA expression coordinated with decreased cell proliferation and increased apoptosis in high dose ETBE and PB groups at week 2 was consistent with our previous results demonstrating that short-term application of 500 ppm PB resulted in cell cycle arrest (Kinoshita et al., 2002). We were able to detect only a slight early increase in PCNA index in high dose ETBE-treated rats and a significant increase in PB-administered rats at week 1. Regenerative cell proliferation after week 2, which is known to occur after induction of apoptosis may be strongly suggested from the present results.

Functions of three "orphan" nuclear receptor superfamily members, designated CAR, PXR/SXR and PPAR, respectively mediating the

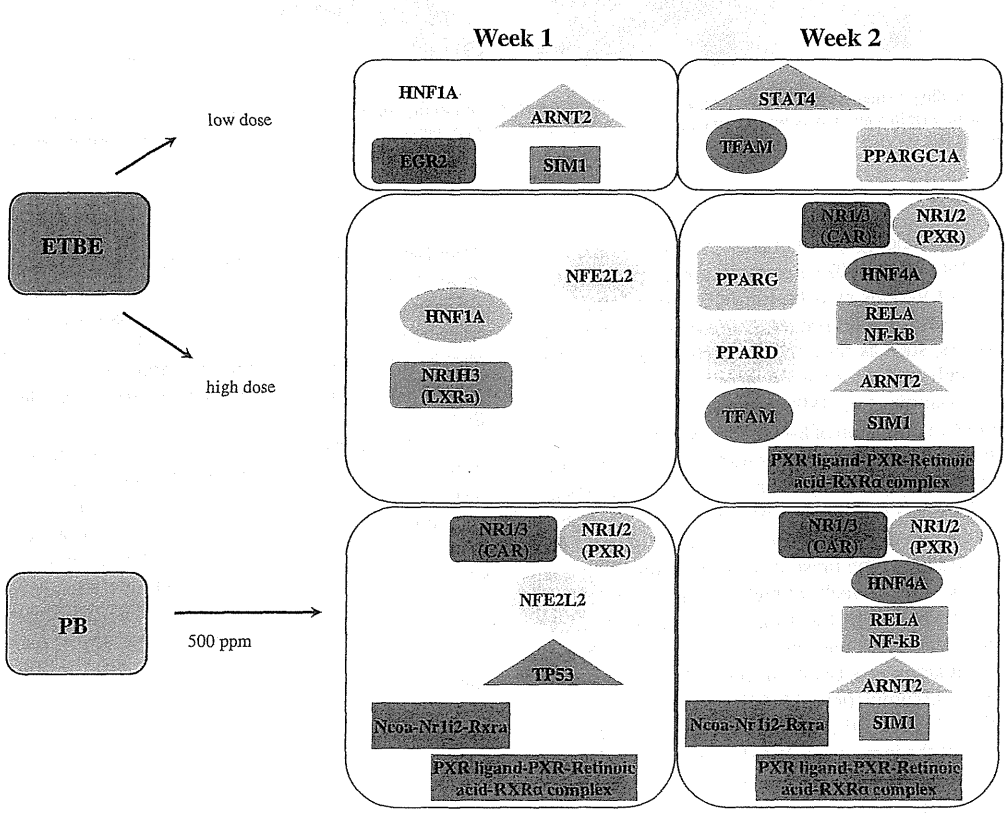

Fig. 2. Summary of comparative analysis of upstream regulators which activation was predicted by IPA analysis (z-score ≥ 2) concerning liver tumorigenicity in rats given low, high dose ETBE or fed a dietary level of 500 ppm PB for 1 and 2 weeks.

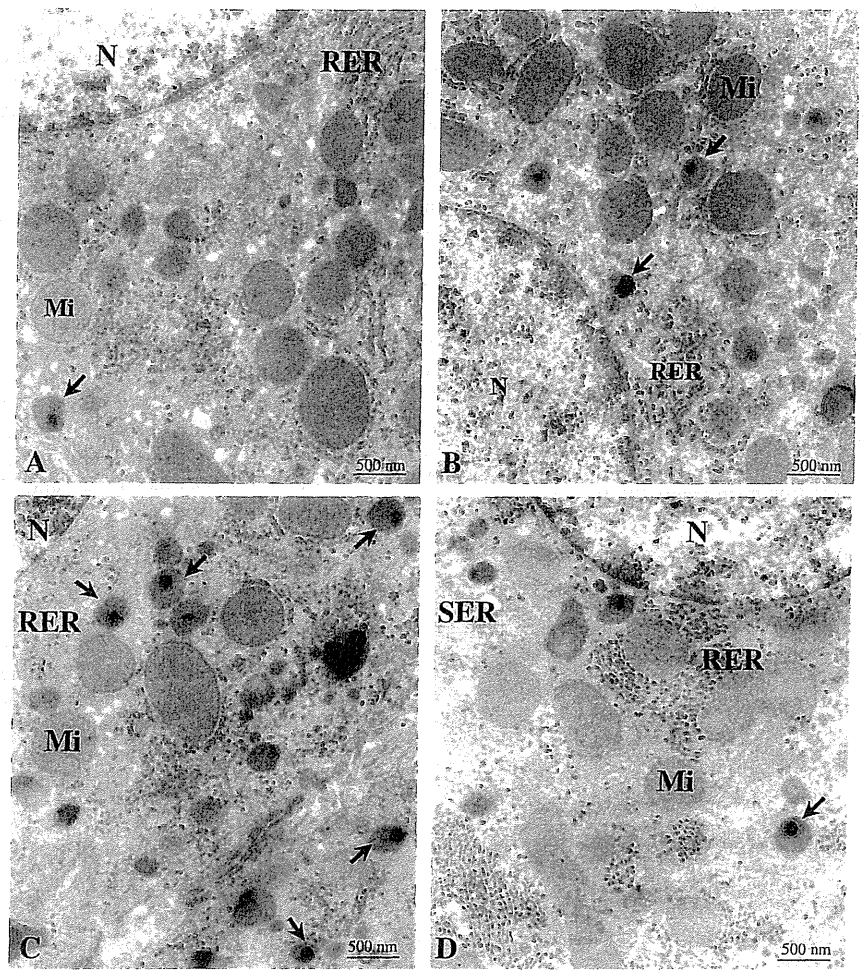

Fig. 3. Representative TEM findings in hepatocytes of F344 rats given ETBE or PB for 2 weeks. Number of peroxisomes in hepatocytes of rats given 0 (control) (A) appeared normal; in low dose ETBE (B) group slight increase in their number was observed, and in high dose ETBE (C) group abundant peroxisomes were obvious (arrows). No peroxisome proliferation was found in hepatocytes of rats fed PB (D).

induction of hepatic CYPs belonging to families CYP2, CYP3, and CYP4 are well recognized (Palut et al., 2002). Reactive oxygen species generated due to induction of various cytochrome P450 isoenzymes, lipid peroxidation and other intracellular processes are involved in regulation of numerous factors, such as transcription factors kappa B, NFkB and AP-1, partly through protein kinase C activation (Brawn et al., 1995; Feig et al., 1994; Klaunig et al., 1998; Storz and Polla, 1996). The dose and time-dependent generation of 8-OHdG, a well-known marker of oxidative DNA damage, has been demonstrated after administration of non-genotoxic carcinogens including chemicals like PB (Kinoshita et al., 2002). Its actual level in the tissue is determined by changes in rates of production of oxygen radicals and its repair (Boiteux and Radicella, 1999; Floyd, 1990). In the present study a significant induction of 8-OHdG formation after 2 weeks of high dose ETBE and PB administrations was coordinated with the suppression of Ogg1 mRNA expression, thus, suggesting that the DNA repair was insufficient, which caused the accumulation of 8-OHdG in the DNA of hepatocytes. Furthermore, coordinated accumulation of 8-OHdG in the nucleus and CYP2B1/2B2 and CYP3A1/3A2 and other CYP isoforms in the cytoplasm of hepatocytes implied that the increase of DNA damage after treatment with ETBE and PB in rats is caused by production of oxidative stress, and is related to increase in P450 protein levels. The levels of 8-OHdG formation in high dose ETBE and PB groups were comparable at week 2. From our previous study, the peak in increase of 8-OHdG formation in the rat liver DNA by 500 ppm PB was observed earlier between 1 and 2 weeks of application, followed by its reduction, as the cells with damaged DNA underwent cell cycle arrest and apoptosis, and their number gradually decreased (Kinoshita et al., 2002). Therefore, it might be suggested that in the present experiment conditions, the peak of 8-OHdG formation in PB group was around days 10–14, while in high dose ETBE group 8-OHdG level was still increasing.

The present data support previous results demonstrating induction of preneoplastic lesions (eosinophilic and basophilic foci) and liver tumors (hepatocellular adenomas; 9 of 50 rats (18%)) by ETBE, which was applied by inhalation exposure at a dose of 5,000 ppm (Saito et al., 2013). In comparison, treatment with PB in diet was shown to result in development of hepatocellular adenoma only in 1 rat of 50 (2%) after 2 years of application (Butler, 1978). The dose of ETBE applied in the present investigation (1000 mg/kg b.w. ×2/day; equal to about 3500 ppm by inhalation treatment, which greatly exceeded the human exposure level) was much higher than that of PB, nevertheless, PB appeared to be the stronger inducer of P450 via CAR and PXR at gene and protein levels. Present results further demonstrated that previously reported promotion effect of ETBE and PB on thyroid tumor development in rats (Hagiwara et al., 2011) is likely to be related to induction of UGT enzymes and their activities by both chemicals, leading to hepatic disposition of T4, which reduces serum T4 concentration, compensatory increase of serum TSH concentration, and finally stimulation of

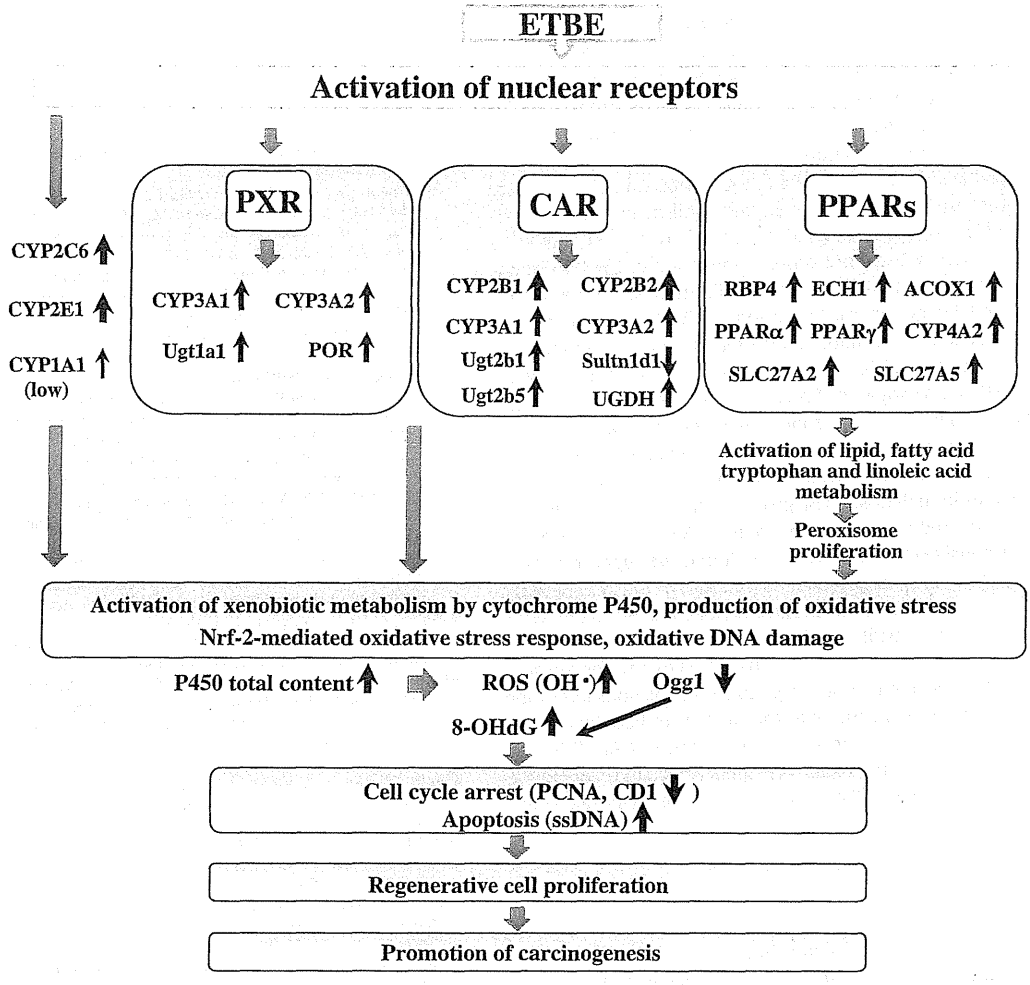

Fig. 4. Graphically illustrated MOA of ETBE hepatocarcinogenicity in rats.

thyroid follicular cell proliferation and ultimately neoplasia. Thus, the MOA for ETBE hepatotumorigenicity basically is likely to be at the same viewpoint as for PB MOA, but existence of some other mechanisms, such as activation of PPARs, may be also suggested. Importantly, it is recognized that the mechanism through the activation of CAR/PXR for PB carcinogenicity in rodents is not relevant to human, since PB is not human carcinogen (La Vecchia and Negri, 2013; Olsen et al., 1993).

The possible adverse effect of ETBE in humans is a public concern, thus, it is very important to assess the human relevance of pharmacokinetics and toxicity data obtained from animals. It has been reported that the biotransformation of ETBE is both qualitatively and quantitatively similar in humans and rats after inhalation exposure under identical conditions (Dekant et al., 2001). The inhalation exposure of 5000 ppm ETBE was shown to exert tumorigenicity in the liver of male rats, while the 1500 ppm dose did not possess any activity (Saito et al., 2013). Furthermore, in initiation–promotion studies, ETBE administered by gavage at a dose of 1000 mg/kg b.w./day but not 300 mg/kg b.w./day was found to exhibit promotional activity (Hagiwara, 2012; Hagiwara et al., 2011). In the present investigation, there was only slight induction of oxidative stress at a low dose of ETBE. These data are supported by our report on initiation/promotion carcinogenicity showing that no-observed-adverse-effect-level (NOAEL) of non-genotoxic chemical ETBE, on promotional activity is 300 mg/kg b.w./day (Hagiwara, 2012; Hagiwara et al., 2011; Suzuki et al., 2012).

Interestingly, results of the proteome, RT-PCR and TEM analyses have suggested that application of high dose ETBE led to PPAR activation in rat livers. Thus, IPA predicted significant activation of PPARγ and PPARδ, and a possibility of PPARα activation dependent of up-regulation PPARs downstream proteins such as CYP4A2 and mitochondrial enzymes involved in fatty acid metabolism (Palut et al., 2002). Furthermore, peroxisome proliferation and PPARα, which is a predominant liver PPAR phenotype expressed in hepatocytes (Holden and Tugwood, 1999; Rao and Reddy, 1987), were induced by high dose ETBE. These results, in coordination with proteome analysis, may be strongly indicative of activation of PPARα as well as PPARγ and PPARδ by ETBE, which may result in oxidative stress and 8-OHdG formation.

PPAR proliferators have been shown to cause liver cancers when chronically administered to rats and mice (Gonzalez and Shah, 2008). In contrast to the results in rodents, there is no evidence that they cause elevated risk of liver cancer or any other neoplasms in humans thus indicating a species difference in the hepatocarcinogenic response. In general, the activation of PPARs in humans seems to have a beneficial effect on health. PPARα activation lowers plasma triglyceride levels and reduces adiposity, which, in turn, improves insulin sensitivity and protects against muscle and hepatic steatosis, including diet-induced steatohepatitis (Berger et al., 2005; Michalik et al., 2006). Ligands for PPARγ have exhibited anticancer effects *in vitro* and *in vivo*, on many tumors including lung, breast, colon, prostate and bladder (Edwards and O'Flaherty, 2008; Han and Roman, 2007). Peroxisome proliferation has not been observed in humans because of much lower levels of PPARα expression as compared with rodents (Yang et al., 2008). Furthermore, mice with human PPARα do not develop hepatocyte hyperplasia while

still mediating many of the functions ascribed to PPARα including hepatocyte hypertrophy (Yang et al., 2008). On the basis of all these data, activation of PPARs, fatty acid metabolism and peroxisome proliferation by ETBE observed in the present study, which was not found with PB, may be one of the mechanisms for ETBE hepatotumorigenicity in rats, but is unlikely to be relevant to humans.

P450 isoenzymes, CYP2A6, CYP3A4 (rat CYP3A2) and CYP2E1 were recently reported to be responsible for metabolism of ETBE to *tert*-butyl alcohol (TBA) in the human liver tissue (Hong et al., 2001; Le Gal et al., 2001). Here, we did not observe induction of CYP2A6 isoenzyme, pointing the existing differences in ETBE metabolizing enzymes in human and rat livers, but the elevation of CYP2E1, an isoenzyme known to be induced by ethanol, supported the data in human. As CYP2E1 was induced in ETBE-treated group, its role in ETBE MOA needs to be further investigated. Previously CAR activation has been shown to induce CYP1A1 in the mouse hepatocytes (Maglich et al. 2002). Since the induction of CYP1A1 was not detected in low dose ETBE-treated rats and only very weak elevations of mRNA and protein levels were obvious in high dose ETBE group, furthermore, its induction in the rat liver appeared to be not dependent of AhR nuclear receptor, as other AhR-responsive elements were not altered, we suggest that observed alteration to CYP1A1 expression plays a minor role in ETBE MOA in the view point of CAR/PXR, or even might not be related to the MOA.

In conclusion, our results indicate that the MOA of ETBE hepatotumorigenicity in rats is similar to that of PB except for the activation of PPARs. The mechanisms are related to conspicuous alteration to DNA oxidative base modifications in the nucleus of hepatocytes via generation of oxidative stress due to the activation of CAR, PXR and PPARs with a sequence of events which presumably lead to regenerative cell proliferation. The MOA of ETBE hepatotumorigenicity in rats is unlikely to be relevant to humans.

Conflict of interest

The sponsor of the study (Petroleum Industry Technology and Research Institute, Inc., Japan) had no influence whatsoever on the results and statements made by the authors in the present study.

Acknowledgments

We thank Azusa Inagaki and Hideki Nakagawa for their technical assistance. This research was sponsored by the Petroleum Industry Technology and Research Institute, Inc., Japan.

References

ACGIH, 2012. Ethyl tert-butyl ether. ACGIH. American Conference of Governmental Industrial Hygienists. Cincinnati, OH. Documentation of the Threshold Limit Values (TLVs) and Biological Exposure Indices (BELs).

Ahmed, F.E., 2001. Toxicology and human health effects following exposure to oxygenated or reformulated gasoline. Toxicol. Lett. 123, 89–113.

Berger, J.P., Akiyama, T.E., Meinke, P.T., 2005. PPARs: therapeutic targets for metabolic disease. Trends Pharmacol. Sci. 26, 244–251.

Boiteux, S., Radicella, J.P., 1999. Base excision repair of 8-hydroxyguanine protects DNA from endogenous oxidative stress. Biochimie 81, 59–67.

Brawn, M.K., Chiou, W.J., Leach, K.L., 1995. Oxidant-induced activation of protein kinase C in UC11MG cells. Free Radic. Res. 22, 23–37.

Butler, W.H., 1978. Long-term effects of phenobarbitone-Na on male Fischer rats. Br. J. Cancer 37, 418–423.

Dekant, W., Bernauer, U., Rosner, E., Amberg, A., 2001. Toxicokinetics of ethers used as fuel oxygenates. Toxicol. Lett. 124, 37–45.

Edwards, I.J., O'Flaherty, J.T., 2008. Omega-3 fatty acids and PPAR gamma in cancer. PPAR Res. 2008, 358052.

Feig, D.I., Reid, T.M., Loeb, L.A., 1994. Reactive oxygen species in tumorigenesis. Cancer Res. 54, 1890s–1894s.

Fenner-Crisp, P.A., Mayes, M.E., David, R.M., 2011. Assessing the human carcinogenic potential of tetrahydrofuran: I. Mode of action and human relevance analysis of the male rat kidney tumor. Regul. Toxicol. Pharmacol. 60, 20–39.

Floyd, R.A., 1990. The role of 8-hydroxyguanine in carcinogenesis. Carcinogenesis 11, 1447–1450.

Funae, Y., Imaoka, S., 1985. Simultaneous purification of multiple forms of rat liver microsomal cytochrome P-450 by high-performance liquid chromatography. Biochim. Biophys. Acta 842, 119–132.

Gluckmann, M., Fella, K., Waidelich, D., Merkel, D., Kruft, V., Kramer, P.J., Walter, Y., Hellmann, J., Karas, M., Kroger, M., 2007. Prevalidation of potential protein biomarkers in toxicology using iTRAQ reagent technology. Proteomics 7, 1564–1574.

Gonzalez, F.J., Shah, Y.M., 2008. PPARalpha: mechanism of species differences and hepatocarcinogenesis of peroxisome proliferators. Toxicology 246, 2–8.

Hagiwara, A., 2012. Threshold level for tumor promotion by ethyl tertiary-butyl ether (ETBE) of hepatic carcinohgenesis in rats. Society of Toxicologic Pathology, Mechanisms of Toxicity, Annual Symposium.

Hagiwara, A., Doi, Y., Imai, N., Nakashima, H., Ono, T., Kawabe, M., Furukawa, F., Tamano, S., Nagano, K., Fukushima, S., 2011. Medium-term multi-organ carcinogenesis bioassay of ethyl tertiary-butyl ether in rats. Toxicology 289, 160–166.

Han, S., Roman, J., 2007. Peroxisome proliferator-activated receptor gamma: a novel target for cancer therapeutics? Anticancer Drugs 18, 237–244.

Holden, P.R., Tugwood, J.D., 1999. Peroxisome proliferator-activated receptor alpha: role in rodent liver cancer and species differences. J. Mol. Endocrinol. 22, 1–8.

Hong, J.Y., Wang, Y.Y., Mohr, S.N., Bondoc, F.Y., Deng, C., 2001. Human cytochrome P450 isozymes in metabolism and health effects of gasoline ethers. Res. Rep. Health Eff. Inst. 7–27 (discussion 95–109).

Kakehashi, A., Inoue, M., Wei, M., Fukushima, S., Wanibuchi, H., 2009. Cytokeratin 8/18 overexpression and complex formation as an indicator of GST-P positive foci transformation into hepatocellular carcinomas. Toxicol. Appl. Pharmacol. 238, 71–79.

Kasai, H., Crain, P.F., Kuchino, Y., Nishimura, S., Ootsuyama, A., Tanooka, H., 1986. Formation of 8-hydroxyguanine moiety in cellular DNA by agents producing oxygen radicals and evidence for its repair. Carcinogenesis 7, 1849–1851.

Kinoshita, A., Wanibuchi, H., Imaoka, S., Ogawa, M., Masuda, C., Morimura, K., Funae, Y., Fukushima, S., 2002. Formation of 8-hydroxydeoxyguanosine and cell-cycle arrest in the rat liver via generation of oxidative stress by phenobarbital: association with expression profiles of p21(WAF1/Cip1), cyclin D1 and Ogg1. Carcinogenesis 23, 341–349.

Klaunig, J.E., Xu, Y., Isenberg, J.S., Bachowski, S., Kolaja, K.L., Jiang, J., Stevenson, D.E., Walborg Jr., E.F., 1998. The role of oxidative stress in chemical carcinogenesis. Environ. Health Perspect. 106 (Suppl. 1), 289–295.

La Vecchia, C., Negri, E., 2013. A review of epidemiological data on epilepsy, phenobarbital, and risk of liver cancer. Eur. J. Cancer Prev. http://dx.doi.org/10.1097/CEJ.0b013e32836014c8.

Le Gal, A., Dreano, Y., Gervasi, P.G., Berthou, F., 2001. Human cytochrome P450 2A6 is the major enzyme involved in the metabolism of three alkoxyethers used as oxyfuels. Toxicol. Lett. 124, 47–58.

Maglich, J.M., Stoltz, C.M., Goodwin, B., Hawkins-Brown, D., Moore, J.T., Kliewer, S.A., 2002. Nuclear pregnane x receptor and constitutive androstane receptor regulate overlapping but distinct sets of genes involved in xenobiotic detoxification. Mol. Pharmacol. 62, 638–646.

Maltoni, C., Belpoggi, F., Soffritti, M., Minardi, F., 1999. Comprehensive long-term experimental project of carcinogenicity bioassays on gasoline oxygenated additives: plan and first report of results from the study on ethyl-tertiary-butyl ether (ETBE). Eur. J. Oncol. 4, 493–508.

McGregor, D., 2006. Methyl tertiary-butyl ether: studies for potential human health hazards. Crit. Rev. Toxicol. 36, 319–358.

McGregor, D., 2007. Ethyl tertiary-butyl ether: a toxicological review. Crit. Rev. Toxicol. 37, 287–312.

Michalik, L., Auwerx, J., Berger, J.P., Chatterjee, V.K., Glass, C.K., Gonzalez, F.J., Grimaldi, P.A., Kadowaki, T., Lazar, M.A., O'Rahilly, S., Palmer, C.N., Plutzky, J., Reddy, J.K., Spiegelman, B.M., Staels, B., Wahli, W., 2006. International Union of Pharmacology. LXI. Peroxisome proliferator-activated receptors. Pharmacol. Rev. 58, 726–741.

Olsen, J.H., Wallin, H., Boice Jr., J.D., Rask, K., Schulgen, G., Fraumeni Jr., J.F., 1993. Phenobarbital, drug metabolism, and human cancer. Cancer Epidemiol. Biomarkers Prev. 2, 449–452.

Omura, T., Sato, R., 1964. The carbon monoxide-binding pigment of liver microsomes. II. Solubilization, purification, and properties. J. Biol. Chem. 239, 2379–2385.

Palut, D., Kostka, G., Strucinski, P., 2002. The role of nuclear receptors in cytochrome P-450 induction by xenochemicals. Rocz. Panstw. Zakl. Hig. 53, 321–332.

Rao, M.S., Reddy, J.K., 1987. Peroxisome proliferation and hepatocarcinogenesis. Carcinogenesis 8, 631–636.

Saito, A., Sasaki, T., Kasai, T., Katagiri, T., Nishizawa, T., Noguchi, T., Aiso, S., Nagano, K., Fukushima, S., 2013. Hepatotumorigenicity of ethyl tertiary-butyl ether with 2-year inhalation exposure in F344 rats. Arch. Toxicol. 87, 905–914.

Storz, G., Polla, B.S., 1996. Transcriptional regulators of oxidative stress-inducible genes in prokaryotes and eukaryotes. EXS 77, 239–254.

Suzuki, M., Yamazaki, K., Kano, H., Aiso, S., Nagano, K., Fukushima, S., 2012. No carcinogenicity of ethyl tertiary-butyl ether by 2-year oral administration in rats. J. Toxicol. Sci. 37, 1239–1246.

Yang, Q., Nagano, T., Shah, Y., Cheung, C., Ito, S., Gonzalez, F.J., 2008. The PPAR alpha-humanized mouse: a model to investigate species differences in liver toxicity mediated by PPAR alpha. Toxicol. Sci. 101, 132–139.

Toxicology and Applied Pharmacology 273 (2013) 1–9

Contents lists available at ScienceDirect

Toxicology and Applied Pharmacology

journal homepage: www.elsevier.com/locate/ytaap

Diphenylarsinic acid, a chemical warfare-related neurotoxicant, promotes liver carcinogenesis *via* activation of aryl hydrocarbon receptor signaling and consequent induction of oxidative DAN damage in rats

Min Wei, Takanori Yamada, Shotaro Yamano, Minoru Kato, Anna Kakehashi, Masaki Fujioka, Yoshiyuki Tago, Mistuaki Kitano, Hideki Wanibuchi *

Department of Pathology, Osaka City University Graduate School of Medicine, 1-4-3 Asahi-machi, Abeno-ku, Osaka 545-8585, Japan

ARTICLE INFO

Article history:
Received 16 July 2013
Revised 20 August 2013
Accepted 20 August 2013
Available online 30 August 2013

Keywords:
Diphenylarsinic acid
Hepatocarcinogenicity
CYP1B1
Oxidative DNA damage
Aryl hydrocarbon receptor
Rat

ABSTRACT

Diphenylarsinic acid (DPAA), a chemical warfare-related neurotoxic organic arsenical, is present in the groundwater and soil in some regions of Japan due to illegal dumping after World War II. Inorganic arsenic is carcinogenic in humans and its organic arsenic metabolites are carcinogenic in animal studies, raising serious concerns about the carcinogenicity of DPAA. However, the carcinogenic potential of DPAA has not yet been evaluated. In the present study we found that DPAA significantly enhanced the development of diethylnitrosamine-induced preneoplastic lesions in the liver in a medium-term rat liver carcinogenesis assay. Evaluation of the expression of cytochrome P450 (CYP) enzymes in the liver revealed that DPAA induced the expression of CYP1B1, but not any other CYP1, CYP2, or CYP3 enzymes, suggesting that CYP1B1 might be the enzyme responsible for the metabolic activation of DPAA. We also found increased oxidative DNA damage, possibly due to elevated CYP1B1 expression. Induction of CYP1B1 has generally been linked with the activation of AhR, and we found that DPAA activates the aryl hydrocarbon receptor (AhR). Importantly, the promotion effect of DPAA was observed only at a dose that activated the AhR, suggesting that activation of AhR and consequent induction of AhR target genes and oxidative DNA damage plays a vital role in the promotion effects of DPAA. The present study provides, for the first time, evidence regarding the carcinogenicity of DPAA and indicates the necessity of comprehensive evaluation of its carcinogenic potential using long-term carcinogenicity studies.

© 2013 Elsevier Inc. All rights reserved.

Introduction

Diphenylarsinic acid (DPAA), an organic arsenical, is a synthetic intermediate as well as a degradation product of chemical warfare agents such as diphenylarsine chloride and diphenylarsine cyanide, which were produced as respiratory irritants during the World Wars I and II (Arao et al., 2009; Haas et al., 1998; Hanaoka et al., 2005). It is generally considered that there are two sources of environmental DPAA: one is the degradation of the above chemical warfare agents abandoned in Japan, Europe and China after World War II (Bunnett and Mikołajczyk, 1998; Kroening, 2011; Stock and Lohs, 1997); another is the illegal dumping of synthetic DPAA itself (Kinoshita et al., 2008). Little was known about the health effects of chronic exposure to DPAA until neurotoxicities—including ataxic gait, titubation, scanning speech, myoclonus and tremors—were reported in inhabitants exposed chronically to DPAA through drinking well water in Kamisu City, Japan (Ishii et al., 2004); the origin of DPAA in Kamisu City well water is suspected to be illegally dumped DPAA that penetrated into the groundwater. Several studies have shown that oxidative and nitrosative stress (Kato et al., 2007) and dysregulation of glutaminase C (Kita et al., 2007) are involved in the neurotoxicites of DPAA.

Inorganic arsenic is a well-known human carcinogen, causing cancers in skin, urinary bladder, and lung and possibly in the liver and kidney in populations chronically exposed through the drinking water (IARC, 2004). Dimethylarsinic acid, a major metabolite of inorganic arsenic in humans, has been demonstrated to induce urinary bladder cancer and promote liver and kidney carcinogenesis in rats, and enhance skin and lung carcinogenesis in mice (Cohen et al., 2006; Wanibuchi et al., 2004). Other organic metabolites of inorganic arsenicals, such as monomethylarsonic acid and trimethylarsine oxide, also exert promotion effects on liver and urinary bladder carcinogenesis in rats (Wanibuchi et al., 2004). The clear carcinogenic potential of

Abbreviations: AhR, aryl hydrocarbon receptor; B[*a*]P, benzo[*a*]pyrene; CYP, cytochrome P450; COX-2, cyclooxygenase-2; DEN, diethylnitrosamine; DMBA, 7,12-dimethylbenz[*a*]anthracene; DPAA, diphenylarsinic acid; GST-P positive foci, glutathione *S*-transferase placental form positive foci; 8-OHdG, 8-hydroxy-2′-deoxyguanosine; PCB, polyhalogenated biphenyl; PCNA, proliferating cell nuclear antigen; TCDD, 2,3,7,8-tetrachlorodibenzo-p-dioxin.

* Corresponding author. Fax: +81 6 6646 3093.
E-mail address: wani@med.osaka-cu.ac.jp (H. Wanibuchi).

0041-008X/$ – see front matter © 2013 Elsevier Inc. All rights reserved.
http://dx.doi.org/10.1016/j.taap.2013.08.022

inorganic arsenic in humans and the ample evidence for the carcinogenicities of organic arsenicals in animal studies have raised serious public concerns about the carcinogenicity of DPAA.

DPAA may be genotoxic: DPAA is negative in the Ames test and *in vivo* micronucleus test (MOEJ, 2012), however, it is positive in the *in vitro* chromosome aberration test (Ochi et al., 2004). Currently, no other information is available for cancer risk assessment of DPAA.

The purpose of the present study was to evaluate modifying effects of DPAA on liver carcinogenesis using a medium-term rat liver carcinogenesis assay. We also examined potential mechanisms by which DPAA could promote carcinogenesis in the rat liver. Herein, we demonstrate that DPAA is a promoter of rat hepatocarcinogenesis and that activation of the aryl hydrocarbon receptor (AhR) signaling pathway is a pivotal mechanism underlying the promotion effects of DPAA: DPAA administered *via* the drinking water (i) increased the transcriptional activity of AhR; (ii) induced expression of the AhR target genes CYP1B1 and COX-2, with the latter possibly being responsible for the observed induction of the anti-apoptotic gene Bcl-2; (iii) promoted oxidative DNA damage; and (iv) enhanced the development of diethylnitrosamine (DEN)-induced preneoplastic lesions in the rat liver.

Materials and methods

Chemicals. Diethylnitrosamine (DEN) was purchased from Tokyo Chemical Industry Co. Ltd., Tokyo, Japan. DPAA was kindly provided by Dr. Kenzo Yamanaka, Department of Biochemical Toxicology, Nihon University College of Pharmacy, Japan. The purity of the DPAA was confirmed to be more than 99.9%, and its stability in tap water for 28 days at room temperature was confirmed using an IC (IC7000, Yokogawa Analytic System Inc., Tokyo, Japan)–ICP-MS (HP 4500, DE, USA) system at Osaka City University Graduate School of Medicine.

Animals. Male F344 rats at 5 weeks of age were obtained from Charles River Japan, Inc. (Atsugi, Shiga, Japan). The animals were housed in polycarbonate cages (5 rats/cage) in experimental animal rooms with a targeted temperature of 22 ± 3 °C, relative humidity of 55 ± 5% and a 12-h light/dark cycle. All animals were acclimated for 7 days before being used for experiments. Diet and drinking water were available *ad libitum* throughout the study. Fresh drinking water containing DPAA was supplied to the animals twice weekly. Body weight and food and water consumption were measured weekly.

Experimental design. The animal experimentation protocols were approved by the Institutional Animal Care and Use Committee of Osaka City University Medical School.

Experiment 1 was designed to determine the effects of DPAA on rat liver carcinogenesis using the medium-term liver bioassay model (also known as the Ito test) (Ito et al., 2003). The selection of DPAA dose was based on the results of a 13-week preliminary study where 6-week old male F344 rats were administered with 0, 12.5, 25, and 50 ppm DPAA in the drinking water. More than 20% suppression of body weight gain was observed in the groups administered with 25 and 50 ppm DPAA from week 4 after treatment, while no suppression of body weight or other toxic signs were observed in the 12.5 ppm DPAA group throughout the study (data not shown). Based on the these results and that the reported maximum concentration of DPAA in drinking well water in DPAA polluted areas was 15 ppm (Ishii et al., 2004; Ishizaki et al., 2005), 20 ppm was determined as the highest dose to be used in the present study. Rats at 6 weeks of age were randomized into 6 groups (Table 1). At the beginning of the study, the rats in groups 1–4 (20 rats each) were given a single intraperitoneal injection of DEN (200 mg/kg body weight, dissolved in 0.9% saline) to initiate liver carcinogenesis, and the rats in groups 5 and 6 (10 rats each) were given saline vehicle alone. Two weeks after initiation, the animals were administered with DPAA in the drinking water for 6 weeks: groups 1–4 received 0, 5, 10, and 20 ppm, respectively, and groups 5 and 6 received 0 and 20 ppm, respectively. All animals were subjected to two-thirds partial hepatectomy at the end of week 3. All surviving rats were terminated by exsanguination *via* transection of the abdominal aorta under deep anesthesia at the end of week 8. At necropsy, livers were excised and weighed, and then 3 slices each from the left lateral, medial, and right lateral lobes were placed in 10% phosphate buffered formalin. Following fixation, liver tissues were embedded in paraffin and processed for histopathological examination and immunohistochemical analysis of glutathione *S*-transferase placental form (GST-P) positive foci, which is a well-established preneoplastic liver lesion in rats (Tsuda et al., 2003), and CYP1B1 and AhR. The remaining liver tissues were flash frozen with liquid nitrogen and stored at −80 °C for mRNA expression analysis, electrophoretic mobility shift assay, and 8-hydroxy-2′-deoxyguanosine (8-OHdG) formation analysis.

Experiment 2 was designed to confirm the effects of DPAA without DEN initiation or partial hepatectomy. Two groups of ten 6-week-old rats were administered DPAA in the drinking water at concentrations of 0 or 20 ppm for 2 weeks (Table 1). At necropsy, liver tissues were processed as in experiment 1 for CYP1B1 and AhR immunohistochemistry, mRNA expression analysis, and electrophoretic mobility shift assay.

Immunohistochemical analysis. Liver specimens were examined for GST-P positive foci formation and CYP1B1 and AhR expression by immunohistochemical staining using the avidin–biotin–peroxidase complex (ABC)

Table 1
Final body weights, liver weights, water, and DPAA intake.

Group	DEN initiation	DPAA (ppm)	No.of rats [a]	Final body weight (g)	Absolute liver weight (g)	Relative liver weight (%)	Average water intake (g/kg body weight/day)	Average DPAA intake (mg/kg body weight/day)
Experiment 1 (8 weeks)								
1	+	0	17	258 ± 14	8.0 ± 0.6	3.1 ± 0.2	96.5	0
2	+	5	20	259 ± 11	8.0 ± 0.4	3.1 ± 0.1	92.4	0.5
3	+	10	16	260 ± 10	8.3 ± 0.6	3.2 ± 0.2	87.4	0.9
4	+	20	17	249 ± 10	8.9 ± 0.7 [b]	3.6 ± 0.2 [b]	81.5	1.6
5	−	0	10	269 ± 12	8.5 ± 0.6	3.2 ± 0.1	93.7	0
6	−	20	9	263 ± 11	9.8 ± 0.7 [c]	3.7 ± 0.3 [c]	79.1	1.6
Experiment 2 (2 weeks)								
1	−	0	10	175 ± 7	5.2 ± 0.4	3.0 ± 0.2	147.9	0
2	−	20	10	158 ± 8 [d]	6.5 ± 0.4 [d]	4.1 ± 0.1 [d]	131.6	2.6

[a] Number of rats that survived to the end of the study.
[b] Significantly different from group 1 at $p < 0.001$ in experiment 1.
[c] Significantly different from group 5 at $p < 0.001$ in experiment 1.
[d] Significantly different from group 1 at $p < 0.001$ in experiment 2.

method. Briefly, paraffin sections were deparaffinized in xylene and then hydrated in graded concentrations of ethanol for 5 min each. Endogenous peroxidase activity was blocked with 0.3% H_2O_2 in distilled water for 5 min, except for CYP1B1 immunohistochemistry. For AhR immunohistochemistry, antigen retrieval was performed by microwaving at 98 °C for 20 min in 0.01 M citrate buffer (pH 6.0) after blocking endogenous peroxidase activity. After blocking non-specific binding with serum at 37 °C for 30 min, sections were incubated with rabbit anti-rat GST-P polyclonal antibody (Medical and Biological Laboratories Co., Ltd., Japan) diluted 1:1000, rabbit anti-human CYP1B1 polyclonal antibodies (H-105, Santa Cruz Biotechnology, Inc., CA, USA) diluted 1:100, or mouse monoclonal [RPT9] aryl hydrocarbon receptor antibody (ab2769, Abcam, Cambridge, MA, USA) diluted 1:125, overnight at 4 °C. Immunoreactivity was detected using VECSTAIN Elite ABC Kit (Vector Laboratories, Burlingame, CA, USA) and 3,3′-diaminobenzidine hydrochloride (Sigma Chemical Co., St Louis, MO, USA) for GST-P and AhR, and VECSTAIN ABC-AP kit (AK-5000) and VECSTAIN AP substrate kit (SK-5100) (Vector Laboratories, Burlingame, CA, USA) for CYP1B1. A primary antibody negative control was included with each staining procedure.

Quantitative analysis of GST-P positive foci in the liver. Numbers and areas of GST-P-positive foci lager than 0.2 mm in diameter and the total areas of liver sections examined were measured blindly using a color image processor (IPAP, Sumica Technos, Osaka, Japan), and the number and area of GST-P positive foci per square centimeter of liver tissue were calculated.

TaqMan real-time quantitative PCR. Total liver RNA was isolated from 7 rats of each group in experiment 1 and 8 rats of each group in experiment 2 using TRIzol® Reagent (Life Technologies, Gaithersburg, MD, USA) according to the manufacturer's instructions. cDNA synthesis was performed with 1 μg of RNA using an Advantage RT-for-PCR kit (Takara Bio, Inc., Otsu, Japan). The mRNA expression levels of 11 cytochrome P450 enzymes in families CYP1-3, proliferating cell nuclear antigen (PCNA) which is a marker of cell proliferation, 3 anti-apoptotic genes (Bcl-2, Mcl-1 and Bcl-xL), and cyclooxygenase-2 (COX-2) were determined by TaqMan real-time quantitative PCR. PCR reagents and sequence-specific primers and probes for each gene (Taqman Gene Expression Assay) were purchased from Applied Biosystems, Inc., CA, USA. mRNA expression assays were performed using a 7500 Fast Real-Time PCR System (Applied Biosystems, Inc., CA, USA) as described previously (Wei et al., 2011). β-actin was employed as an internal control. Serially diluted standard cDNAs were included in each Taqman PCR reaction to create standard curves. The amounts of gene products in the test samples were estimated relative to the respective standard curves. Values for target genes were normalized to those for β-actin.

Electrophoretic mobility shift assay. Electrophoretic mobility shift assay (EMSA) was carried out to determine the effect of DPAA on AhR transcriptional activity. Nuclear extracts were prepared from the liver tissues of 2 rats of each group in experiments 1 and 2 using Nuclear Extraction Kit according to the manufacture's instruction (Panomics, Fremont, CA). EMSA were carried out using EMSA "Gel Shift" kit (Panomics, Fremont, CA, USA) according to the manufacturer's protocol. Briefly, 12 μg of nuclear protein were incubated with a biotin-labeled oligonucleotide containing the consensus binding sequence for AhR/Arnt (5′-GGGGA TCGCGTGACAACCC-3′) for 30 min at 15 °C, and then transcription factor-bound oligonucleotide was separated from unbound oligonucleotide by electrophoresis on a 6% nondenaturing polyacrylamide gel. DNA–protein complexes were transblotted to Biodyne B nylon membrane (Pall Corporation, Ann Arbor, MI) and then fixed by a UV crosslinker. The signals were detected by Streptavidin-HRP-based chemiluminescence provided in the EMSA "Gel Shift" kit and visualized using an LAS-3000 Image Reader (Fuji Photo Film, Tokyo, Japan).

Detection of oxidative damage in the liver DNA. Formation of 8-OHdG in liver DNA, a marker of oxidative DNA damage (Dizdaroglu et al., 2002), was determined by high-performance liquid chromatography with electrochemical detection as described previously (Wei et al., 2009).

Statistical analysis. All mean values are reported as mean ± SD. Statistical analyses were performed using the Statlight program (Yukms Co., Ltd., Tokyo, Japan). Homogeneity of variance was tested by the F-test or Bartlett test. Differences in mean values between the DEN initiation alone group and groups initiated with DEN and followed with various dose of DPAA in experiment 1 were evaluated by the 2-tailed Dunnett test when variance was homogeneous and the 2-tailed Steel test when variance was heterogeneous. Differences in mean values between the non-treatment control and 20 ppm DPAA group in experiments 1 and 2 were evaluated by the Student's *t*-test when variance was homogeneous and Welch's *t*-test when variance was heterogeneous. p values less than 0.05 were considered significant.

Results

Survival, food and water consumption, DPAA intake, and body and organ weights

The number of rats surviving to the end of the study, final average body and liver weights, and average water and DPAA intake in experiment 1 are summarized in Table 1. Three, four, three and one rat died in groups 1, 3, 4 and 6, respectively. All these rats died within one week after partial hepatectomy, possibly due to operation-related reasons, and therefore are not included in the analyses. All the remaining animals survived to the end of study in good condition. No clinical signs or symptoms of neurotoxicity were observed in any of the DPAA-treated rats throughout the study. DPAA had no significant effects on the body weights irrespective of DEN initiation. Among the DEN-initiated groups, absolute and relative liver weights of the 20 ppm DPAA group (group 4) were significantly higher than that of the DEN alone group (group 1). Significant increases in both absolute and relative liver weights were also observed in the 20 ppm DPAA alone group (group 6) compared to the non-initiated control group (group 5). The intake of DPAA was approximately proportional to the doses administered in the drinking water, although, water intake tended to decrease in the DPAA-treated groups compared to the controls (Table 1). Food consumption was similar among the groups (data not shown). Mild bile duct hyperplasia was observed in the livers of the 20 ppm DPAA groups, irrespective of DEN initiation, but no liver tumors were found in any of the groups.

In experiment 2, in contrast to experiment 1, administration of 20 ppm DPAA in the drinking water resulted in a significant suppression of weight gain. A possible explanation for this discrepancy is that the average intake of DPAA by the rats in experiment 2 (2.6 mg/kg body weight/day) was much greater than that by rats in experiment 1 (1.6 mg/kg body weight/day) (Table 1). This could be due to the fact that the rats in experiment 1 were treated with DPAA from 8 weeks of age while the rats in experiment 2 were treated with DPAA from 6 weeks of age; consequently, the rats in experiment 2 were younger and smaller than the rats in experiment 1. As expected, 20 ppm DPAA significantly increased both the absolute and relative liver weights compared to the control.

GST-P positive foci formation in livers

In experiment 1, GST-P positive foci developed in the livers of DEN-initiated rats. As shown in Fig. 1, among the DEN-initiated groups, both total number and average area of GST-P positive foci per unit area of the rat livers were significantly increased in the 20 ppm DPAA ppm group compared to the DEN alone group, while 5 and 10 ppm DPAA had no

effect on the formation of GST-P positive foci. In the non-initiation groups, no GST-P positive foci were observed in either the control or the 20 ppm DPAA group. In experiment 2, there were no GST-P positive foci in either the control group or the 20 ppm DPAA group.

Expression of CYP enzymes and oxidative DNA damage in livers

To identify possible CYP enzymes that may be responsible for the metabolism of DPAA, we first determined the mRNA expression of 11 CYP enzymes in families CYP1-3 in the rat livers in experiment 1. As summarized in Table 2 and shown in Fig. 2A, 20 ppm DPAA significantly induced the expression of CYP1B1 in the livers, irrespective of DEN initiation. In contrast, 20 ppm DPAA significantly suppressed the expression of CYP1A2, CYP2A2, CYP2C2, CYP3A1, and CYP3A2 and had no effect on the expression of CYP1A1, CYP2A1, CYP2B1, CYP2B2, or CYP2E1, irrespective of DEN initiation (Table 2, Supplementary Fig. 1). DPAA at the doses of 5 and 10 ppm had no effect on the expression level of any of the above CYPs.

The finding that CYP1B1 is the only CYP enzyme that is elevated in response to DPAA treatment, suggests that CYP1B1 might be responsible for DPPA metabolism. This result also suggests the existence of active metabolites of DPAA in the livers. Therefore, we assessed the formation of 8-OHdG, one of the most abundant oxidative lesions in DNA generated by reactive oxidative stress (Dizdaroglu et al., 2002), in the rat livers in experiments 1. As shown in Fig. 2B, 8-OHdG was significantly increased in the liver DNA of the 20 ppm DPAA group, but not the 5 or 10 ppm DPAA groups, irrespective of DEN initiation.

To confirm the effects of DPAA on the expression of CYPs, the expression of the 11 CYP enzymes analyzed in experiment 1 were analyzed in the livers of rats treated with 20 ppm DPAA without DEN initiation or partial hepatectomy (experiment 2). In experiment 2, as observed in experiment 1, expression of CYP1B1 was significantly increased by 20 ppm DPAA (Table 2 and Fig. 3A). Immunohistochemical staining of CYP1B1 in control rats was characterized by weak staining of the cytoplasm of centrilobular hepatocytes (Fig. 3B-I). Expression of CYP1B was markedly increased in the livers of rats treated with 20 ppm DPAA and characterized by strong staining in the centrilobular hepatocytes and moderate staining in other areas of the lobule (Fig. 3B-II). The effect of 20 ppm DPAA on the expression of the other CYP enzymes in experiment 2 was mostly similar to its effect in experiment 1: the expression of CYP1A2, CYP2A2, CYP2C2, CYP3A1 and CYP3A2 was decreased and the expression of CYP2A1, CYP2B1 and CYP2B2 was not affected

Table 2
mRNA expression of CYP enzymes in the livers of rats.

	Experiment 1 Fold changes (vs. DEN alone)			Fold changes (vs. 0 ppm DPAA)	Experiment 2 Fold changes (vs. 0 ppm DPAA)
DEN initiation	+	+	+	−	−
DPAA (ppm)	5	10	20	20	20
CYP1A1	1.0 [a,b]	1.0	1.2	1.3	0.4*
CYP1A2	0.9	1.0	0.6*	0.7*	0.3***
CYP1B1	1.0	1.0	8.0**	10.8**	7.8***
CYP2A1	1.0	0.8	0.9	1.1	1.1
CYP2A2	1.0	0.9	0.6*	0.5*	0.4***
CYP2B1	1.0	1.1	0.9	1.0	1.1
CYP2B2	1.2	1.2	0.9	1.0	1.1
CYP2C2	1.1	1.1	0.4*	0.1***	0.03***
CYP2E1	0.9	1.0	0.8	0.9	0.6**
CYP3A1	1.0	1.0	0.5*	0.7*	0.6**
CYP3A2	0.8	0.8	0.5*	0.4**	0.5*

Significantly different from their respective controls at *$p < 0.05$; **$p < 0.01$; ***$p < 0.001$.
[a] The data is shown as fold change relative to the control.
[b] Data presented as mean ± SD is shown in Figs. 2, 3, and Supplementary Figs. 1 and 2.

(Table 2, Supplementary Fig. 2). However, the expression levels of CYP1A1 and CYP2E1 were significantly suppressed by 20 ppm DPAA in experiment 2 while their expression levels were not changed in experiment 1 (Table 2, Supplementary Fig. 2). This discrepancy is possibly due to the increased intake of DPAA in experiment 2 compared to experiment 1 as discussed above.

Activation of AhR signaling pathway in livers

Since the induction of CYP1B1 has generally been linked with activation of AhR and most compounds that are known to induce CYP1B1 have been shown to be ligands for AhR (Nebert and Dalton, 2006; Tsuchiya et al., 2003), we assessed the effects of DPAA treatment on AhR transcriptional activity in rat livers. Electrophoretic mobility shift assays revealed that following DEN initiation (experiment 1 rats), DPAA caused an apparent elevation of the nuclear AhR/ARNT DNA-binding complex at 20 ppm, but not at 5 or 10 ppm (Fig. 4A). The nuclear AhR/ARNT DNA-binding complex was also markedly increased in the

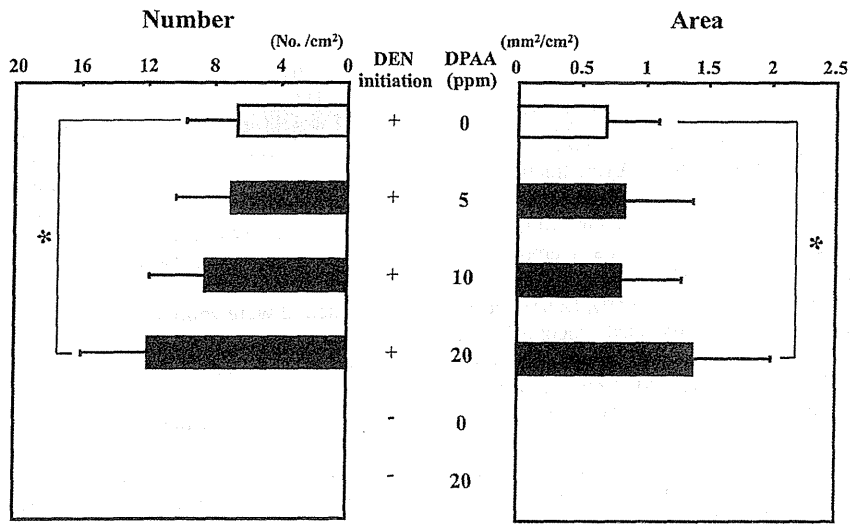

Fig. 1. Numbers and areas of the preneoplastic lesion GST-P-positive foci in rat livers in the medium-term rat liver carcinogenesis assay (experiment 1). DPAA at the dose of 20 ppm significantly increased both the numbers and areas of GST-P-positive foci in livers. *Significantly different from the DEN alone group at $p < 0.01$.

livers of experiment 2 rats treated with 20 ppm DPAA (Fig. 4B). Furthermore, immunohistochemical staining revealed that AhR was observed in the nuclei of only a few hepatocytes in the centrilobular area in the control rats (Fig. 4C-I), while strong nuclear expression of AhR was observed in the livers of rats treated with 20 ppm DPAA, especially in the centrilobular hepatocytes (Fig. 4C-II). These results suggest that the transcriptional activity of AhR was increased by treatment with 20 ppm DPAA. It is notable that the expression pattern of CYP1B1 and AhR are similar in the livers and is correlated to GST-P positive foci, which mainly developed in the centrilobular area (Supplementary Table 1).

To determine the effects of activation of the AhR signaling pathway by DPAA on apoptosis and cell proliferation, mRNA expression of Bcl-2, COX-2, Mcl-1 and Bcl-xL, and PCNA in the livers was analyzed. In experiment 1 rats, 20 ppm DPAA, but not 5 or 10 ppm DPAA, significantly increased the expression of Bcl-2 and COX-2, irrespective of DEN initiation (Figs. 2C and D). A significant increase in the expression of Mcl-1 was observed in the 20 ppm group compared to the control in the non-initiation groups, but not in the DEN-initiation groups (Fig. 2E). In experiment 2 rats, expression of Bcl-2, COX-2, and Mcl-1 were significantly increased in the 20 ppm DPAA group (Figs. 2C,D and 3E, respectively). DPAA had no effect on the expression of PCNA in either experiment 1 rats (Fig. 2F) or experiment 2 rats (Fig. 3F). DPAA also did not have an effect on the expression of Bcl-xL in either experiment 1 rats (Supplementary Fig. 1) or experiment 2 rats (Supplementary Fig. 2).

Discussion

The results of this study demonstrate that DPAA, a neurotoxicant of humans, is a promoter of hepatocarcinogenesis in rats, as evidenced by the finding that it significantly enhanced the development of DEN-induced GST-P positive foci, which is a well-established preneoplastic liver lesion in rats and has been accepted as a reliable and sensitive end-point marker in assessment of the hepatocarcinogenic effects of environmental chemicals (Tsuda et al., 2003). We also found that DPAA is an activator of AhR. Activation of AhR is linked with induction of the xenobiotic metabolizing enzyme CYP1B1 (Nebert and Dalton, 2006; Tsuchiya et al., 2003), and elevated expression of CYP1B1 may contribute to the increased oxidative DNA damage observed in the livers of DPAA treated rats. DPAA treatment also induced the expression of Bcl-2 possibly *via* induction of COX-2 (Breinig et al., 2007; Kern et al., 2006; Sheng et al., 1998), which is an AhR target (Degner et al., 2007; Wolfle et al., 2000), thereby increasing the resistance of these cells to apoptosis. These findings provide, for the first time, evidence for carcinogenic effects of DPAA and indicate that activation of AhR may play a vital role in the promotion effects of DPAA on rat hepatocarcinogenesis.

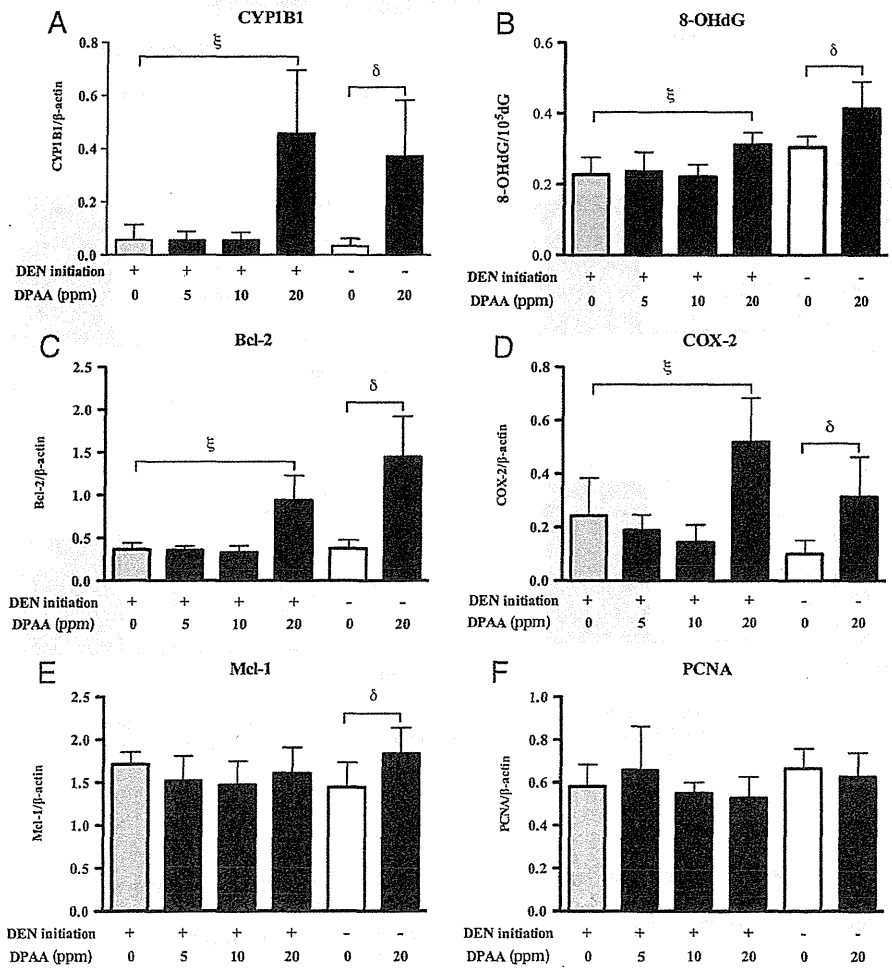

Fig. 2. mRNA expression and oxidative DNA damage in rat livers in the medium-term rat liver carcinogenesis assay (experiment 1). (A) CYP1B1, (B) formation of 8-OHdG in rat liver DNA. (C) Bcl-2, (D) COX-2, (E) Mcl-1, (F) PCNA. §Significantly different from the DEN alone group (DEN initiation +; 0 ppm DPAA) at $p < 0.01$, $p < 0.05$, $p < 0.01$, $p < 0.05$ in A, B, C and D, respectively. $^{\delta}$Significantly different the non-treatment control group (DEN initiation −; 0 ppm DPAA) at $p < 0.01$, $p < 0.05$, $p < 0.001$, $p < 0.01$ and $p < 0.05$ in A, B, C, D and E, respectively.

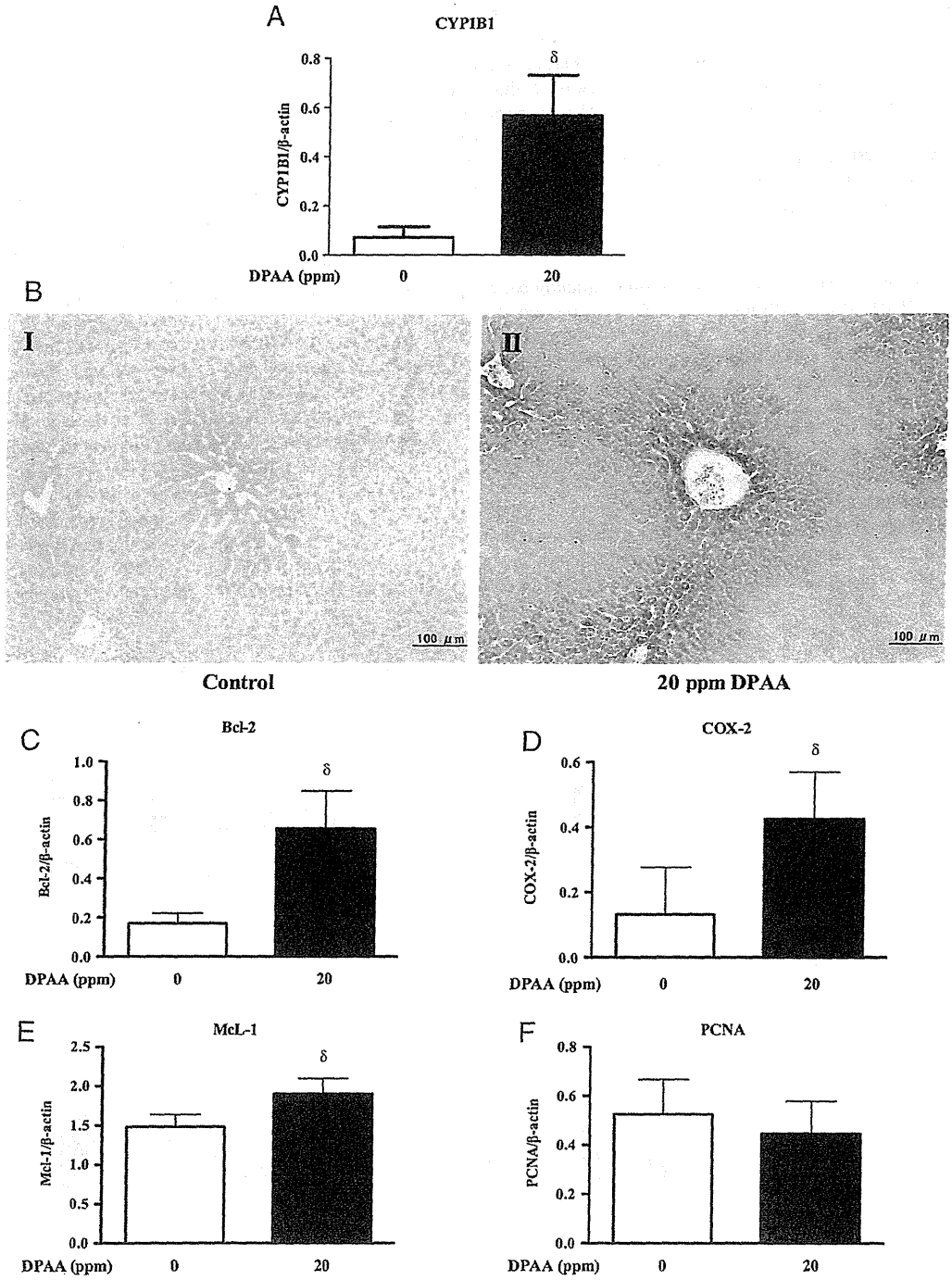

Fig. 3. mRNA expression and immunohistochemical staining of CYP1B1 in rat livers in the 2-week DPAA treatment experiment (experiment 2). (A) mRNA expression of CYP1B1, (B) immunohistochemical staining of CYP1B1, (C) Bcl-2, (D) COX-2, (E) Mcl-1, (F) PCNA. [δ]Significantly different from the control group (0 ppm DPAA) at $p < 0.001$, $p < 0.0001$, $p < 0.05$, and $p < 0.001$ in B, C, D and E, respectively.

AhR is a ligand-activated cytoplasmic transcription factor, and is known to be activated by a number of environmental carcinogens such as 2,3,7,8-tetrachlorodibenzo-*p*-dioxin (TCDD), polycyclic aromatic hydrocarbons (*e.g.* benzo[*a*]pyrene (B[*a*]P), 7,12-dimethylbenz[*a*]anthracene (DMBA), polyhalogenated biphenyls (PCBs)) (Marlowe and Puga, 2005; Safe, 1994; Shimada and Fujii-Kuriyama, 2004). Upon activation, AhR translocates into the nucleus and forms a transcriptionally active heterodimer with ARNT that enhances transcription of various genes including enzymes involved in xenobiotic metabolism such as CYP1A1 and CYP1B1. These xenobiotic metabolizing enzymes are capable of converting the above carcinogens into the highly oxidized metabolites relevant to their carcinogenicities (Denison et al., 2011; Marlowe and Puga, 2005; Nebert and Dalton, 2006; Shimada and Fujii-Kuriyama, 2004). In the present study, CYP1B1 is the only CYP enzyme induced by DPAA treatment, and its induction is accompanied by increased nuclear expression and transcriptional activity of AhR.

These findings suggest that AhR-regulated CYP1B1 might be an essential metabolic activation enzyme of DPAA. Further study is necessary to measure the effects of DPAA on the activity of CYP1B1 and clarify the exact role of CYP1B1 in the metabolism of DPAA.

The fact that DPAA did not induce CYP1A1, a target of other AhR ligands such as TCDD and DMBA, suggests a preferential gene tropism for DPAA-activated AhR. It is known that even in the same cell lineage, different ligands for AhR can lead to different patterns of gene expression that are determined by the core sequence of the AhR responsive element in the promoter region of the target genes and the different sets of transcription cofactors recruited by AhR (Beischlag et al., 2002; Denison et al., 2011; Matikainen et al., 2001; Nebert and Dalton, 2006). In the present study, considering that decreased mRNA expression of multiple CYP isoforms belonging to CYP subfamilies 1–3 was observed, the decreased CYP mRNA synthesis could be due, at least in part, to the hepatocytotoxicity of DPAA.

Recently, Naranmandura et al. identified a new urine metabolite of DPAA and suggested the existence of a hydroxylated aromatic that could be formed by oxidation of DPAA by cytochrome P450 in the rat liver (Naranmandura et al., 2009). These results taken together with our findings of coupled induction of CYP1B1 and increased 8-OHdG formation raise the possibility that CYP1B1 may be involved in the generation of oxidative DNA damage and this may contribute to the promotion effects of DPAA on rat liver carcinogenesis.

Although the mechanism of action of AhR has been extensively studied, the exact molecular events that result in AhR-dependent carcinogenic effects remain unclear (Denison et al., 2011). Anti-apoptotic effects have been linked to the promotion effects of the AhR ligand TCDD on rat hepatocarcinogenesis (Chopra and Schrenk, 2011; Luebeck et al., 2000; Stinchcombe et al., 1995). Activation of AhR by TCDD has also been shown to inhibit apoptosis in rat primary hepatocytes and several human non-tumorigenic and cancer cell lines (Davis et al., 2003; Schrenk et al., 2004; Vogel et al., 2007). In human lymphoma cell lines, induction of anti-apoptotic Bcl-2 family members are responsible for the anti-apoptotic effect of TCDD-activated AhR, and these alterations are associated with overexpression of cyclooxygenase-2 (COX-2) (Vogel et al., 2007). COX-2 is one of the target genes of AhR (Degner et al., 2007; Wolfle et al., 2000) and has been demonstrated to confer increased resistance to apoptosis *via* induction of Bcl-2 in colon and liver cancers (Breinig et al., 2007; Kern et al., 2006; Sheng et al., 1998). In the present study, DPAA, at the dose that activated AhR and exerted promotion effects (20 ppm), significantly increased the expression of both Bcl-2 and COX-2 irrespective of DEN initiation. Mcl-1 was also significantly induced in the livers of rats administered 20 ppm DPAA without DEN initiation, however, interestingly, its expression was not affected in the livers of rats administered DPAA after DEN-initiation. We tried to compare quantitatively the number of apoptotic cells by TdT-mediated dUTP nick end labeling assay in the livers of the rats in experiment 1, but the method failed due to the extremely low number of positive cells in the livers of these rats (data not shown). Nevertheless, our results imply that the anti-apoptotic effects of DPAA on initiated cells is mediated by AhR, and that induction of COX-2 and Bcl-2 may contribute to the promotion effects of DPAA in the liver.

In the present study, activation of AhR, increased expression of AhR target genes (CYP1B1, COX-2), induction of oxidation DNA damage, and increased GST-P positive foci formation were consistently observed only in the livers of rats treated with 20 ppm DPAA, but not in rats treated with 10 ppm or 5 ppm DPAA. These findings suggest that the promotion effects of DPAA on rat hepatocarcinogenesis are concomitant with AhR activation and that, therefore, AhR activation plays a pivotal role in the promotion effects of DPAA.

The effects of DPAA were only observed at the relatively high dose of 20 ppm. This dose is close to the maximum exposure level of human beings to DPAA (15 ppm) (Ishii et al., 2004; Ishizaki et al., 2005). The fact that a DPAA effect was observed at 20 ppm but not 10 ppm, indicates that the range between carcinogenic and non-

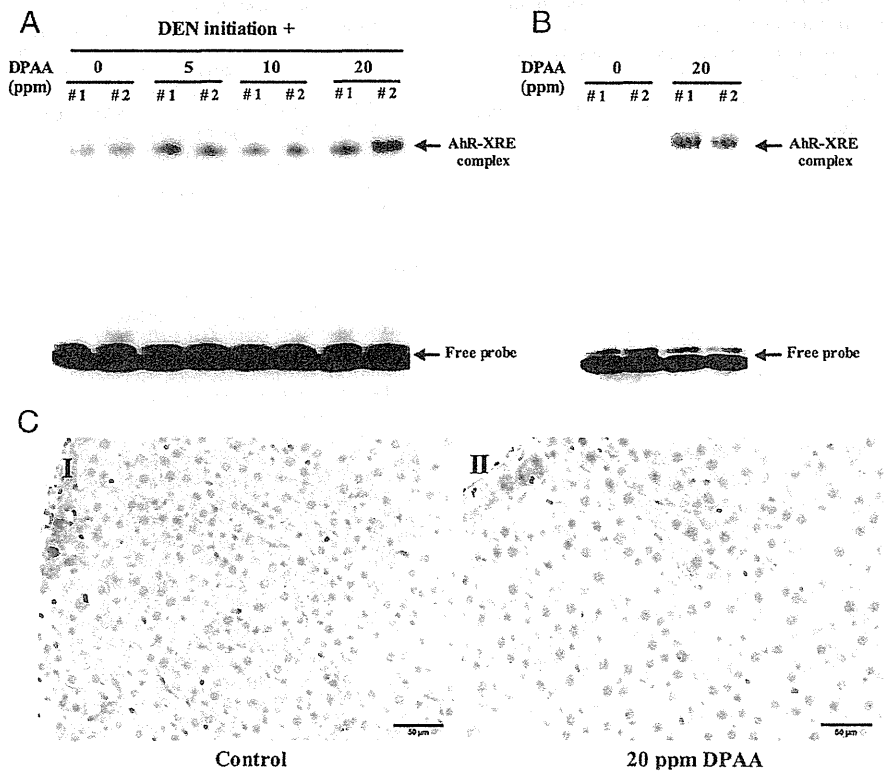

Fig. 4. Electrophoretic mobility shift assay to examine the effects of DPAA on AhR activation in experiments 1 (A) and 2 (B), and immunohistochemical staining of AhR in experiment 2 (C).